SUSY Higgs at the LHC: Large stop mixing effects and associated production

G. Bélanger[1], F. Boudjema[1], and K. Sridhar[2]

1. Laboratoire de Physique Théorique LAPTH [1]
Chemin de Bellevue, B.P. 110, F-74941 Annecy-le-Vieux, Cedex, France.
2. Department of Theoretical Physics, Tata Institute of Fundamental Research
Homi Bhabha Road, 400 005 Mumbai, India

Abstract

We revisit the effect of the large stop mixing on the decay and production of the lightest SUSY Higgs at the LHC. We stress that whenever the inclusive 2-photon signature is substantially reduced, associated production, Wh and $t\bar{t}h$, with the subsequent decay of the Higgs into photons is enhanced and becomes an even more important discovery channel. We also point out that these reductions in the inclusive channel do not occur for the smallest Higgs masses where the significance is known to be lowest. We show that in such scenarios the Higgs can be produced in the decay of the heaviest stop. For not too heavy masses of the pseudo-scalar Higgs where the inclusive channel is even further reduced, we show that large stop mixing also allows the production of the pseudo-scalar Higgs through stop decays. These large mixing scenarios therefore offer much better prospects than previously thought. As a by-product we have recalculated $\tilde{t}_1\tilde{t}_1^*h$ production at the LHC and give a first evaluation of the $\tilde{t}_1\tilde{t}_1^*Z$.

LAPTH-730/99
TIFR/TH/99-17
Apr. 1999

1 Introduction

The most popular alternative to the Standard Model, $\mathcal{SM}$, is supersymmetry which at the moment fits in very well with all the precision data. So well in fact that some see in the latest precision data as preferring a low Higgs mass a very good evidence for SUSY. In fact a low mass for one of the *scalar* Higgses is the most robust limit of any supersymmetric model, contrary to all the other (s)particles of the model which may have rather high masses. In the minimal scenario of SUSY, the light Higgs mass can not exceed ~ 130GeV. Considering the existing LEP2[1] direct searches which indicate a mass greater than about 90GeV means that the lightest SUSY Higgs is confined to a small mass range. Yet this range of Higgs masses poses considerable problems for hadron colliders. For a review see[2]. The dominant decay into $b\bar{b}$ is not exploitable, especially in the *inclusive* production channel $gg \to h \to b\bar{b}$, due to the huge QCD background. One therefore has to rely on the much smaller two-photon signal[3]. However, especially for the LHC, the two-photon decay of the light Higgs to which dedicated detectors are being designed constitutes a challenge. Moreover many effects either due to the direct[4, 5, 6] or indirect (loop)[5, 7, 8, 9] contributions of the rich SUSY spectrum enter the predictions of the two-photon rate of the supersymmetric Higgs. These can lead to a substantial reduction of the supersymmetric Higgs signal as compared to the standard model Higgs. Take for instance the rather simple scenario [5, 10] where all sparticles, apart from the parameters of the Higgs sector, are very heavy and where mixing effects are negligible. This is the scenario which has been extensively investigated by the ATLAS[11, 12]/CMS[13] collaborations which leads to the much celebrated $M_A - \tan\beta$ Higgs discovery potential of the LHC. For short, we will refer to this model as Class-H scenario. In this scenario the two-photon Higgs signal can be much reduced compared to the $\mathcal{SM}$ Higgs especially as one lowers the mass of the pseudo-scalar boson, A^0. Nonetheless, even in this scenario, this channel covers a large part of the $M_A - \tan\beta$ discovery plane, while when M_A gets small so that the two-photon signal gets too small, one can extend the discovery potential by exploiting the signatures of the then not too heavy additional Higgses [10, 11, 12, 13]. It is therefore important to inquire how much the important two-photon signal can get reduced and equally important to investigate when this reduction occurs, whether new mechanisms for Higgs production open up or are enhanced. Could the latter then make up for the loss in the former?

Considering that a general SUSY model furnishes an almost untractable number of parameters to give an unambiguous answer, apart from the Class-H scenario only partial investigations[7, 8, 9] within specific models have been conducted. To quantify how the rate of the two-photon signal can be affected as the SUSY parameters are varied, it is

instructive to take as a reference point the signal for a $\mathcal{SM}$ Higgs with a mass that of the lightest SUSY Higgs. In[8] this has been done within the mSUGRA hypothesis[14] but considering only the dominant inclusive Higgs production channel: $gg \to h \to \gamma\gamma$. One does find indeed that this ratio can be much smaller than unity even for relatively large M_A (which is generic in mSUGRA) and hence making it more difficult to search for the SUSY Higgs than for the same mass $\mathcal{SM}$ Higgs. However it is known[15] that within mSUGRA other channels for Higgs production may open up, like the cascading of the heavier neutralino to a lighter one and a Higgs, thus offering the fantastic possibility of not only discovering supersymmetry but allowing an easy detection of the Higgs[16] before its observation in the two-photon channel. Recently, it has been argued[9], that even in the large M_A region, the so-called decoupling limit[17], if one introduces large mixing in the stop sector a very substantial *reduction* can also ensue in the *inclusive* two-photon Higgs signal. This effect together with the issue of the mixing in the Higgsinos/gaugino sector had been studied previously by comparing the rates with and without mixing[7]. It was found that there were small regions in parameter space where the rate for the two-photon Higgs signal could be either very much *reduced* or very much *enhanced* by the inclusion of mixing.

When large reductions in an important channel occur it is crucial to find out how other channels are affected. What has not been stressed in the previous studies[7, 8, 9], especially in the case of large mixing, is the importance of the associated Higgs production[18, 19, 20] and even if no efficient b-tagging were possible, how in these scenarios these processes can salvage the Higgs signal. Within the $\mathcal{SM}$ and in the no-mixing scenarios, both CMS[21, 13] and ATLAS[22, 12] have now shown that associated Higgs production (Wh, Zh and $t\bar{t}h$), with the subsequent decay of the Higgs into photons, can provide an invaluable Higgs signal, when enough luminosity has been accumulated. This is because, although associated production has lower rates than the inclusive channel, the corresponding signals are not plagued by as much background. The CMS analysis[13] for the $\mathcal{SM}$ Higgs shows that already with an integrated luminosity of $30 fb^{-1}$ the $\gamma\gamma l$ ($l = e, \mu$) leads to a significance higher than 5 (thus an observable Higgs signal) for the range of light Higgs masses we are interested in. For a high luminosity of $100 fb^{-1}$ this significance improves to more than 10 and is higher than the significance in the inclusive channel for practically all Higgs masses in the range of interest. Although it is known that the ATLAS analyses are less optimistic[2] when it comes to the two-photon signal, either in the associated or inclusive channel[12], it remains that at high luminosity the associated production provides a better reach in the $M_A - \tan\beta$ plane[12]. One should therefore also inquire in the case of the SUSY Higgs if the rates for associated production are reduced

[2]The differences between ATLAS and CMS are quantified in [23].

together with the inclusive rates or if they can rather help the discovery potential. At the same time if the rates for the SUSY Higgs are very much affected this generally means that some sort of non-decoupling of some of the SUSY particles is taking place. These particles should then be observed directly. Moreover since their coupling to the Higgs can not be negligible, these same particles could trigger Higgs production, through their decays for instance or through new associated productions. Another important aspect to address is the impact of stop mixing on the Higgs mass and its conjunction with the reduction in the inclusive channel. Indeed, the significance in the inclusive two-photon channel is very much dependent on the Higgs mass, even in the narrow range allowed by SUSY[12, 13], contrary to the associated two-photon channel where the significances are rather flat as a function of the Higgs mass in the range of interest[13, 12].

The present paper revisits the case of the large mixing in the stop sector[7, 9], how the Wh/Zh and $t\bar{t}h$ associated production saves the day when the inclusive channel drops to critical levels and how other new channels for Higgs production open up. To set the stage, section 2 is intended as a reminder of how much a reduction in the usual light Higgs signals can occur and is tolerable in the Class-H scenario. This will serve as a benchmark when we study whether the other scenarios could give reductions which are much worse than those obtained with lowering M_A, a situation of some concern especially if no new production mechanism is exploitable. We will also present some approximations for evaluating the reductions due to M_A which will be useful even when we study the stop mixing case.

Our analysis of the large mixing scenario in the stop sector is contained in Section 3. We first consider the large M_A limit. While we confirm that large reductions in the inclusive channel can occur, we point out that in most cases these are no worse than what is obtained with a low M_A in the no-mixing case. Moreover we will show that if $\tan\beta > 3$ an increase in the *inclusive* channel is possible. This increase is not possible for low values of $\tan\beta$ as studied in [9] because the effect is associated with a too low Higgs mass already excluded by LEP2. We also carefully analyse for which (light) Higgs masses these reductions occur. We will show that contrary to the no-mixing scenario where the signals in the inclusive channels are lowest for the lowest Higgs masses, in the case of large stop mixing the most drastic drops in the inclusive channels do not occur for the lightest Higgs mass possible. Indeed the effect of mixing tends to increase the mass of the Higgs compared to its value in the absence of mixing. Considering that the significances for the $\mathcal{SM}$ Higgs in the inclusive channel are lowest for the lowest possible Higgs masses in our range, $\sim 90 - 130$GeV, means that the largest reductions do not necessarily correspond to the lowest Higgs signal. For instance a reduction of .4 may well be tolerated for a Higgs mass of 110GeV but a reduction of .8 may be "too much"

when it occurs in conjunction with $m_h = 90$GeV. More importantly we find that at the same time as the inclusive channel decreases, the associated production increases and has much better significances than with a $\mathcal{SM}$ Higgs or with a corresponding SUSY Higgs where the stop mixing have been switched off. We will explain why this is so. It should also be pointed out that the large reductions in the inclusive channel occur mostly when one of the stops becomes rather light, below about 200GeV. In many instances, as first suggested by [24], associated $\tilde{t}_1\tilde{t}_1 h$ production can provide a new channel to search for the light Higgs. We will quantify how much one can benefit from this additional channel. Most studies [7, 9] have assumed equality of all soft squark masses which almost invariably leads to a maximal mixing angle $|\sin 2\theta_{\tilde{t}} = 1|$, where $\theta_{\tilde{t}}$ is the mixing angle in the stop sector. Maximal mixing should be viewed as a very special singular point in the large array of the SUSY parameters and even though justified for the first two families as suggested by the mSUGRA[14] scenario is quite unnatural for the third family especially in view of the large Yukawa coupling. We show, nonetheless, that maximal mixing is not always required for the reductions in the two-photon rates to occur. However, moving away even slightly from this singular mixing angle, while not changing much the previous conclusions, can open yet another Higgs production channel. We point out that provided $m_{\tilde{t}_2}$ is not too large, say $m_{\tilde{t}_2} \leq 500$GeV, so that its production rate is large, $\tilde{t}_2$ can provide a source of Higgs through its decay into the lighter stop thanks to a sizeable Yukawa $\tilde{t}_2\tilde{t}_1 h$ coupling. This coupling is controlled by the same parameters that make the $\tilde{t}_1\tilde{t}_1 h$ coupling large and which lead to a reduction of the inclusive channel. We will compare the rate for this new Higgs production mechanism $\sigma(pp \to \tilde{t}_2\tilde{t}_2^* \to \tilde{t}_2\tilde{t}_1^* h + \tilde{t}_2^*\tilde{t}_1 h)$ with the associated lightest stop pair production mechanism $\sigma(pp \to \tilde{t}_1\tilde{t}_1^* h)$ [24] and show that the cascade decay of the $\tilde{t}_2$ can be substantial. This is akin[15] to the mixing in the higgsino-gaugino sector which has been shown[16] to allow a direct Higgs production through the cascade decay $\chi_2^0 \to \chi_1^0 h$. We then move to the analysis of the combined effect of allowing for smaller pseudo-scalar masses together with large stop mixing. For moderate M_A our conclusions are little changed, the associated productions offering always a good channel. When M_A gets rather small ($M_A \sim 250$GeV), the usual reduction, as compared to the $\mathcal{SM}$, in both the inclusive and associated production occurs. This is irrespective of mixing and can be explained along the lines of what happens in the Class-H scenario. Including the large mixing effects from the stops could decrease even further the signal from the inclusive channel, but the same effect again helps increase the associated production channel. Therefore the reach in this channel alone is better than what previously studied by ATLAS[12, 11] and CMS[13] in the $M_A - \tan\beta$ plane for the no-mixing Class-H scenario. Luckily in these situations with both a low M_A and large mixings in the stop sector we find that beside the new channels for Higgs (h) production $\sigma(pp \to \tilde{t}_2\tilde{t}_2 \to \tilde{t}_2\tilde{t}_1 h)$ and $\sigma(pp \to \tilde{t}_1\tilde{t}_1^* h)$, one can also have $\sigma(pp \to \tilde{t}_2\tilde{t}_2 \to \tilde{t}_2\tilde{t}_1 A)$. There

are even instances where the pseudo-scalar Higgs triggers h production through $A \to Zh$. Independently of the extreme mixing scenario studied here we advocate to exploit the potentially large Yukawa coupling of the stops to search for the Higgs(es) through the cascade decays of these third generation squarks. In all our discussion we do not mention rescuing the Higgs signal through its decay into $b\bar{b}$ in the associated production[25] which would be possible provided good b-tagging is available as discussed by ATLAS[26, 12]. This is a difficult issue [27] especially at high luminosity and further simulation studies are needed. Section 4 gives our conclusions.

2 A warm up: Variation with M_A in the case of no mixing

In order to compare the various effects of lowering the masses of the SUSY particles, we start by briefly reviewing the situation when the masses of all sparticles but those of the Higgs sector are set to a high scale, $\tilde{M}_S = 1TeV$. The mass of the pseudo-scalar Higgs is let free. Moreover in the illustration we have also taken the Higgs mixing parameter such that $\mu = -180GeV$ and the $SU(2)$ gaugino mass $M_2 = 500$GeV with the traditional GUT assumption on the gaugino masses which at the electroweak translates as

$$M_1 = \frac{5}{3} \tan^2 \theta_W M_2 \tag{2.1}$$

Therefore strictly speaking we have allowed rather light charginos and neutralinos. All the tri-linear A-terms were set to zero. These kind of scenarios[5, 10, 11, 13], with high masses of sfermions, have been assumed in the simulation searches for the Higgs(es) by the ATLAS/CMS Collaboration leading to the much advertised $M_A - \tan\beta$ plots. Meanwhile it has been known for some time that as M_A increases one reaches a decoupling regime[17] whereby at low energy only the lightest neutral Higgs appears in the spectrum with the important property that its couplings are essentially the same as those of the standard model. This kind of $\mathcal{SM}$-like Higgs should be easiest to discover at the LHC. However as the mass of the pseudoscalar decreases the production rates of the lightest Higgs also decrease. The reduction in the inclusive two-photon rate of the Higgs, as compared to the $\mathcal{SM}$, is defined through the ratio

$$R_{gg\gamma\gamma} = \frac{\Gamma^{SUSY}(h \to gg) \times BR^{SUSY}(h \to \gamma\gamma)}{\Gamma^{SM}(h \to gg) \times BR^{SM}(h \to \gamma\gamma)} \tag{2.2}$$

This ratio is calculated by taking the *same mass* for the $\mathcal{SM}$ Higgs as the one that is derived for the SUSY Higgs once all the SUSY parameters are set. Throughout this

paper we use HDECAY[28] to calculate all the couplings, widths and branching ratios of the Higgs. This program incorporates the leading two-loop corrections for the Higgs masses following[29]. We show in Fig. 1 how this ratio decreases with M_A. This ratio can drop to as little as $\sim 30\%$ for $M_A = 200$GeV and $\tan\beta = 10$. Though trivial in this case, it is useful to point for later that as the pseudo-scalar Higgs mass decreases so do the other Higgs masses[3], therefore the most drastic drops occur for the lowest range of the lightest Higgs, see Fig. 2. This is particularly drastic for $\tan\beta = 2.5$GeV, where the drop occurs around $m_h \sim 90$GeV. It is for these low masses that the significance of the $\mathcal{SM}$ Higgs is also lowest[11, 13] and therefore for this low $\tan\beta$ this would constitute the worst scenario for the discovery of the lightest SUSY Higgs through its two-photon decay[4].

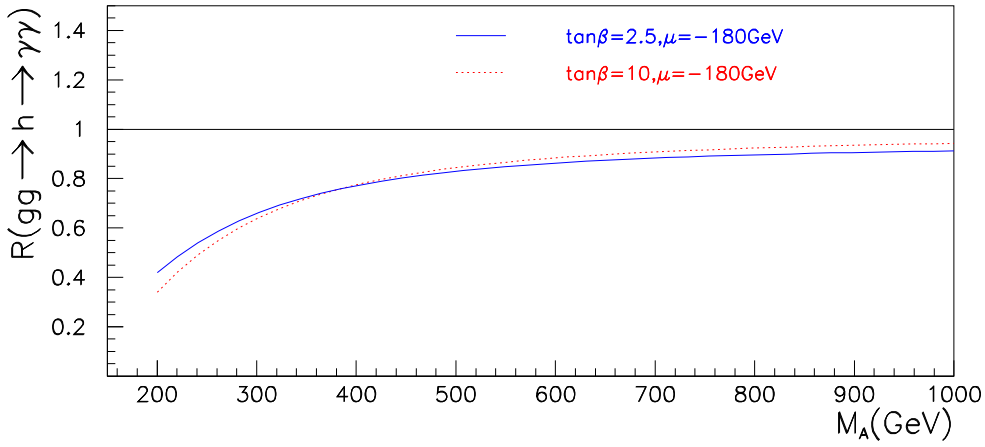

Figure 1: *Variation of* $R_{gg\gamma\gamma}$ *with* M_A*, for* $\tan\beta = 2.5$ *(full) and* $\tan\beta = 10$ *(dotted)*

What is troublesome for a low M_A is that the branching fraction into two photons is the main reason behind the drop, as shown in Fig. 2. This ratio is defined as

$$R_{\gamma\gamma} = \frac{BR^{SUSY}(h \to \gamma\gamma)}{BR^{SM}(h \to \gamma\gamma)} \tag{2.3}$$

For instance for $M_A = 200$GeV and $\tan\beta = 2.5$, the ratio of the branching fraction into photons, $R_{\gamma\gamma}$, is reduced to about .5 with respect to what it would be in the $\mathcal{SM}$. This reduction accounts for much of the reduction in $R_{gg\gamma\gamma}$, $R_{gg\gamma\gamma} = .4$. Therefore one expects also a considerable drop in the Higgs signal even in the associated channel Wh and $t\bar{t}h$ with the subsequent decay of the Higgs into two photons. These channels have been shown to be invaluable[22, 11, 12, 13] especially when a high luminosity has been accumulated.

[3] In the analysis we have required $M_h > 90$GeV.

[4] Of course, for $M_A \leq 2m_t$ there is a chance of discovering the other Higgses.

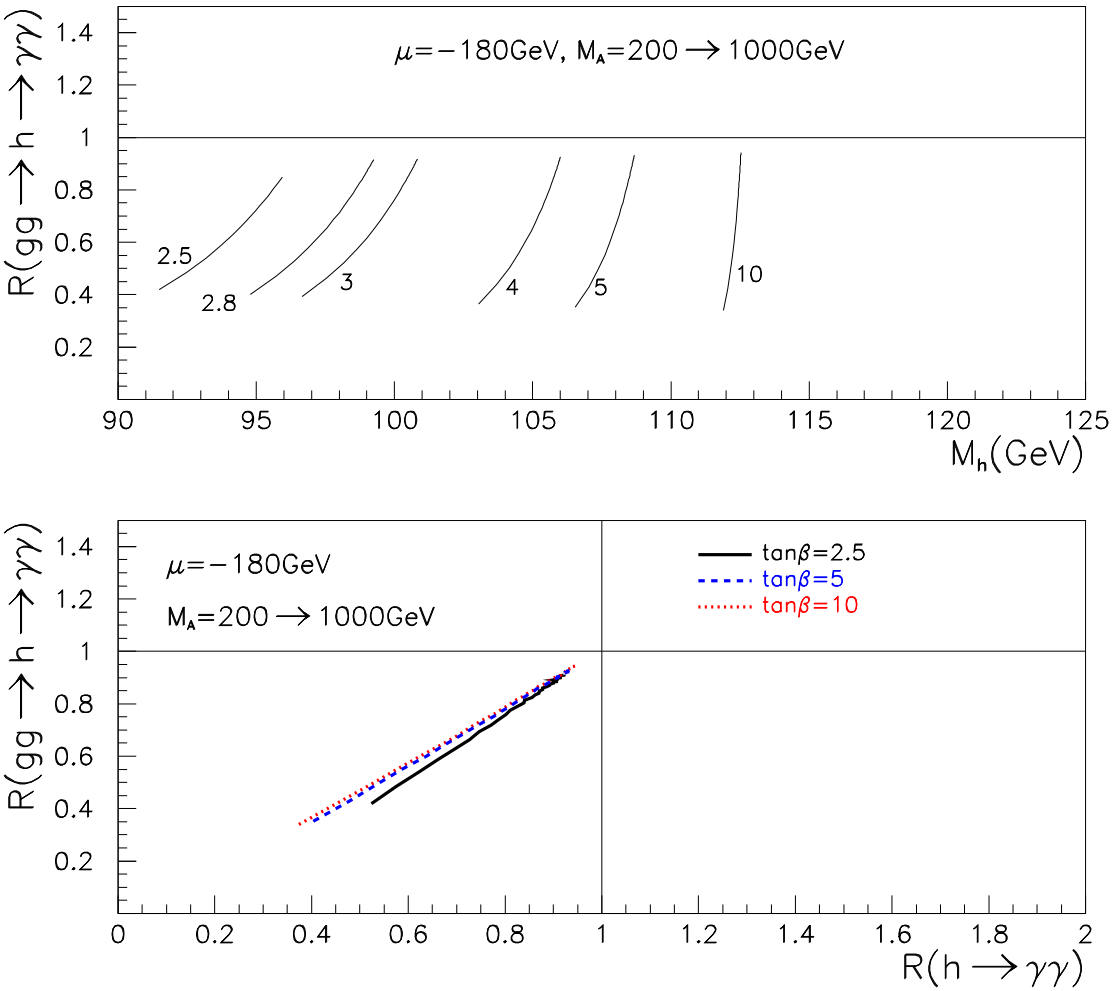

Figure 2: *a)* $R_{gg\gamma\gamma}$ *vs* M_h *as* M_A *varies from 200GeV to 1000GeV for different values of* $\tan\beta$. $\mu = -180 GeV$. *The lowest values of* $R_{gg\gamma\gamma}$ *and* $R_{\gamma\gamma}$ *correspond to* $M_A = 200 GeV$. *b)* $R_{gg\gamma\gamma}$ *vs* $R_{\gamma\gamma}$.

To get an understanding of these gross features and compare with what happens in other scenarios, it is worth discussing how the various couplings, $t\bar{t}h$, $b\bar{b}h$ and Wh/Zh that enter both the associated production and, at the loop level, the inclusive production are influenced by a change in M_A. This is best illustrated and most transparent in the large M_A, so-called decoupling, limit which has been shown to be already operative at 200GeV[17]. Take the $t\bar{t}h$ coupling which differs from the $\mathcal{SM}$ by the factor R:

$$V_{tth} = \frac{g}{2M_W} R\, m_t \quad \text{with} \quad R = \frac{\cos\alpha}{\sin\beta} \tag{2.4}$$

where α is the usual angle that appears in the diagonalization of the CP-even neutral Higgs mass matrix. As was shown elsewhere[30, 31], in this limit and *up to radiative*

corrections we may introduce the factor r

$$\tan\alpha\tan\beta = -(1+r) \quad \text{with} \quad r \ll 1 \tag{2.5}$$

where r collects all M_A dependence and other radiative corrections which also occur in the computation of the Higgs masses. Neglecting the latter we have

$$r \simeq \frac{2M_Z^2}{M_A^2}\,\frac{\tan^2\beta - 1}{\tan^2\beta + 1} \geq 0 \tag{2.6}$$

then the *reduction* factor which appears in $t\bar{t}h$ is

$$R^2 = \frac{1+\tan^2\beta}{1+\tan^2\beta + r^2 + 2r} \qquad R \simeq 1 - \frac{r}{1+\tan^2\beta} \tag{2.7}$$

Likewise it is found that in $h\bar{b}b$ there is an *enhancement* factor which especially, for larger values of $\tan\beta$, is more substantial than the reduction in the top vertex

$$R_{bbh} \simeq 1 + r\frac{\tan^2\beta}{1+\tan^2\beta} \tag{2.8}$$

On the other hand the WWh/ZZh vertex, controlled by $\sin(\alpha-\beta)$, is much less affected: it only shows a *quadratic* dependence in r:

$$R_{VVh} \simeq 1 \; - \; \frac{r^2}{2}\frac{\tan^2\beta}{(1+\tan^2\beta)^2} \tag{2.9}$$

In the $\mathcal{SM}$ $\Gamma(h\to\gamma\gamma)$ is dominated by the W loop which interferes destructively with the top. Since, in this scenario the dominant W coupling is hardly affected at moderate M_A the little change in the top (bottom) coupling has negligible effect on $\Gamma(h\to\gamma\gamma)$. However this is not the case for the branching fraction into photons. Here, since the total width is dominated by the width into $b\bar{b}$, which is larger than in the $\mathcal{SM}$, the branching ratio into photons will be reduced, especially as $\tan\beta$ increases, see Eq. 2.8. On the other hand we expect a slight decrease in the $\Gamma(h\to gg)$. This is because it is dominated by the top loop in the $\mathcal{SM}$, and therefore it is reduced roughly as the $t\bar{t}h$ vertex is reduced. Therefore the main effect in the production rate $pp\to h\to\gamma\gamma$ is due to the reduction in $Br(h\to\gamma\gamma)$. This very crude argument gives the correct order of magnitude in the different drops in $R_{gg\gamma\gamma}$ and $R_{\gamma\gamma}$ shown in the figures. Writing for example

$$R_{\gamma\gamma} \simeq 1 \; - \; \frac{\Gamma^{SM}(h\to b\bar{b})}{\Gamma^{SUSY}(h\to b\bar{b})} \simeq 1 - \frac{4M_Z^2}{M_A^2}\frac{\tan^2\beta(\tan^2\beta-1)}{(1+\tan^2\beta)^2} \tag{2.10}$$

we recover $R_{\gamma\gamma} = .483$ for $M_A = 200\text{GeV}$ and $\tan\beta = 2.5$ which compares very well with the full calculation. Moreover in a first approximation, the change in the width into

gluons can be mostly accounted for by the change in the $t\bar{t}h$ vertex. In which case we may write

$$R_{gg\gamma\gamma} \simeq 1 - \frac{4M_Z^2}{M_A^2}\frac{\tan^2\beta - 1}{1+\tan^2\beta} \tag{2.11}$$

For larger $\tan\beta$ and especially for low values of M_A the approximation is acceptable but not as good. This is partly due to the effect of radiative corrections on the $h \to b\bar{b}$ coupling through the diagonalisation of the neutral Higgs mass matrices[5]. Especially for large $\tan\beta$ these corrections are no longer so suppressed compared to the M_A^2 corrections [8, 32, 31, 33]. In our case the effect is rather marginal since the only mixing parameter, μ, is rather small compared to the SUSY scale. However let us stress that in all the analyses in this paper even when considering large values of the tri-linear coupling (see next section) the branching ratio into $b\bar{b}$ is hardly affected. Because our aim is to concentrate on the effect of the tri-linear coupling of the top sector we do not, in the present paper, analyse the case with very large $\tan\beta$ as these would require to analyse the sbottom sector and also for large μ possible reductions in the $h \to b\bar{b}$ branching ratio.

When considering the associated channels, beside the reduction in the two-photon branching ratio, a further, even though slight, reduction factors affects $t\bar{t}h$ production while we expect Wh to be much less affected. This is borne out by the numerical analysis shown in Fig. 1-3. Once again we define, for the associated productions, ratios normalized to the $\mathcal{SM}$ rates for the same Higgs mass:

$$R_{W\gamma\gamma} = \frac{\sigma^{SUSY}(pp \to Wh) \times BR^{SUSY}(h \to \gamma\gamma)}{\sigma^{SM}(pp \to Wh) \times BR^{SM}(h \to \gamma\gamma)} \tag{2.12}$$

and similarly for the associated top production: $R_{tt\gamma\gamma}$. At the level of the cross sections, $\sigma(pp \to Wh, Zh, t\bar{t}h)$, the ratios are assumed to be given by the ratios of the squares of the WWh and $t\bar{t}h$ couplings. We clearly see, Figs. 1-3, that a lowering of M_A in case of no mixing not only results in a lowering of m_h but also in a reduction of *both* the inclusive and associated two photon channels, as compared to the $\mathcal{SM}$ signal for the same m_h. The worst hit channels are the direct production and the $t\bar{t}h$. The Wh channel is slightly less affected. Note that $t\bar{t}\gamma\gamma$ *vs* $R_{gg\gamma\gamma}$ shows almost no $\tan\beta$ dependence, Fig. 3. This is due to the dominance of the top loop in the $gg \to h$ production, controlled by the same vertex that enters the associated $t\bar{t}h$ cross section. These reductions occur for the lightest Higgs mass and are due essentially to the drop in the branching ratio of the Higgs into two photons, see Figs. 1-3. Since as we pointed earlier the significances in the associated channels are rather flat with respect to the Higgs mass in the range we are interested in, this explains why the 5σ discovery region based on the associated channel in

[5]In this discussion this applies especially to the off-diagonal terms of the Higgs mass matrix.

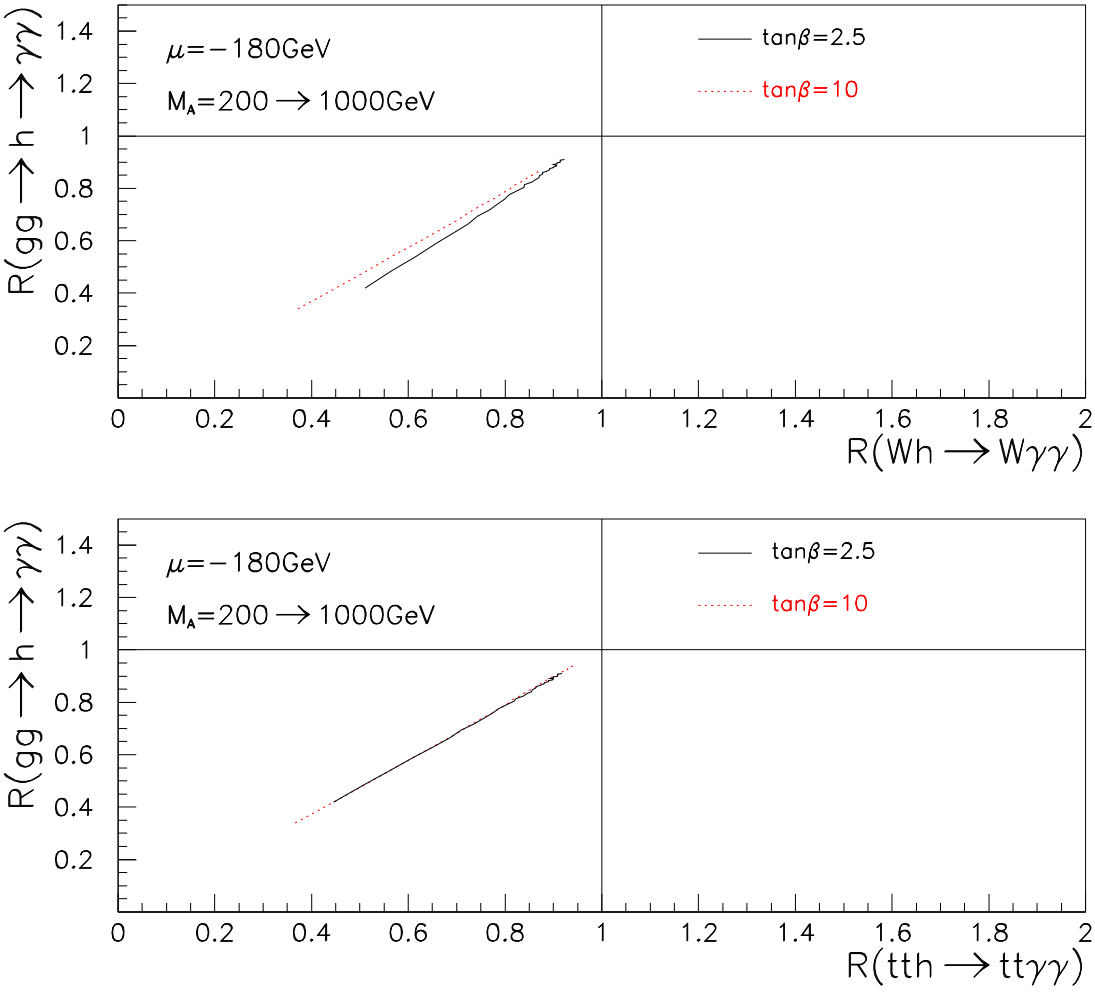

Figure 3: *Variation of* $R_{gg\gamma\gamma}$ *vs* $R_{W\gamma\gamma}$-$R_{t\bar{t}\gamma\gamma}$ *with* $200 \leq M_A \leq 1000\,GeV$ *and* $\tan\beta = 2.5(full), 10(dotted)$.

the $M_A - \tan\beta$ plane[11, 13] are almost independent of $\tan\beta$ ($2.5 \leq \tan\beta \leq 10$). On the other hand the discovery region based on the inclusive channel shows a strong difference between low and high $\tan\beta$ values. This is due essentially to the low significances for low Higgs masses which translates into low significances for $\tan\beta$ in case of no mixing for a fixed value of M_A. Therefore although the *reduction* due to a low M_A is slightly worse for $\tan\beta = 10$ than for $\tan\beta = 2.5$, Fig. 1, the significance in the direct channel is much better for $\tan\beta = 10$ ($m_h \sim 110$GeV) for $\tan\beta = 2.5$ ($m_h \sim 93$GeV). This observation is to be kept in mind and shows the importance of localising where in terms of m_h any reduction, especially, in the inclusive direct channels occurs. Take for instance the CMS analysis[13]. It is found that already with a low luminosity of 30fb^{-1} the significance for the $\mathcal{SM}$ Higgs is larger in the associated channel than in the inclusive channel for $m_h < 105$GeV and is above 5. Translated to Class-H this means that for $M_A \geq 450$GeV associated production allows observability of the light Higgs for all values $\tan\beta = 2.5 - 10$ whereas direct production extends the reach in M_A for $\tan\beta = 10$ ($M_A \sim 400$GeV). With a higher luminosity of 100fb^{-1}, the CMS analysis shows that the reach in M_A is better in the associated channel for all values of $\tan\beta$ and especially for low $\tan\beta$. In terms of the ratio $R_{\gamma\gamma}$, this analysis translates into discovery for $R_{\gamma\gamma} > .4$ corresponding to $M_A > 220$GeV (even slightly better for $\tan\beta = 2.5$, see Fig. 3). Note that one can recover the obsvervability region of the SUSY Higgs of the CMS analysis by combining our results for the ratios R with their analysis for the $\mathcal{SM}$. As stated earlier the ATLAS[12] analysis requires higher luminosities and the above numbers correspond roughly to a luminosity of 300fb^{-1} to take full advantage of the associated production[6].

3 Mixing in the stop sector

To discuss the stop sector and define our conventions, we turn to the weak eigenstate basis where the mass matrix in the $\tilde{t}_L, \tilde{t}_R$ involves the SUSY soft-breaking masses: the common $SU(2)$ mass $\tilde{m}_{\tilde{Q}_3}$ and the $U(1)$ mass $\tilde{m}_{\tilde{U}_{3R}}$, beside the mixing, $\tilde{m}^2_{\tilde{t}_{LR}}$

$$
\begin{aligned}
m^2_{\tilde{t}_L} &= \tilde{m}^2_{\tilde{Q}_3} + m_t^2 + \frac{1}{2}M_Z^2(1 - \frac{4}{3}\sin^2\theta_W)\cos(2\beta) && (3.13)\\
m^2_{\tilde{t}_R} &= \tilde{m}^2_{\tilde{U}_{3R}} + m_t^2 + \frac{2}{3}M_Z^2\sin^2\theta_W\cos(2\beta) \\
m^2_{\tilde{t}_{LR}} &= -m_t(A_t + \frac{\mu}{\tan\beta}) \equiv -m_t\tilde{A}_t && (3.14)
\end{aligned}
$$

[6]For lower luminosities the ATLAS significances in the associated channels are based on a Poisson statistics. We thank Guillaume Eynard for providing us with his code and the "data" for the SM Higgs in the separate channels Wh/Zh and $t\bar{t}h$, see also [22].

One sees that apart from the soft SUSY-breaking parameters: $\tilde{m}_{\tilde{Q}_3}$, $\tilde{m}_{\tilde{U}_{3R}}$ and the tri-linear top term (A_t), there appears also the ubiquitous $\tan\beta$ and the higgsino mass term μ.

The stop mass eigenstates are defined through the mixing angle $\theta_{\tilde{t}}$, with the lightest stop, $\tilde{t}_1$,

$$\tilde{t}_1 = \cos\theta_{\tilde{t}}\ \tilde{t}_L + \sin\theta_{\tilde{t}}\ \tilde{t}_R \tag{3.15}$$

It is quite useful to express the mixing angle as[34, 35]:

$$\tan(2\theta_{\tilde{t}}) = \frac{-2m_t\tilde{A}_t}{\tilde{m}^2_{\tilde{Q}_3} - \tilde{m}^2_{\tilde{U}_{3R}} + \frac{M_Z^2\cos 2\beta}{2}(1-\frac{8s_W^2}{3})} \quad \text{or} \quad \sin(2\theta_{\tilde{t}}) = \frac{2\ m^2_{\tilde{t}_{LR}}}{m^2_{\tilde{t}_1} - m^2_{\tilde{t}_2}} \tag{3.16}$$

For further reference note, in the case of equal soft SUSY breaking masses for the left and right sector of the stop ($\tilde{m}^2_{\tilde{Q}_3} = \tilde{m}^2_{\tilde{U}_{3R}}$), that apart from the case of extremely small mixing $\tilde{A}_t = \mathcal{O}(M_Z/10)$, one has maximal mixing: $\sin(2\theta_{\tilde{t}}) \simeq 1$. In this case we have

$$\tan(2\theta_{\tilde{t}}) \simeq \frac{m_t}{M_Z}\frac{12\tilde{A}_t}{M_Z}\frac{\tan\beta^2+1}{\tan\beta^2-1} \tag{3.17}$$

3.1 The $\tilde{t}_1\tilde{t}_1 h$ vertex

Mixing in the stop sector not only allows one of the stops to be rather light, but this light stop can have rather large Yukawa couplings. Let us therefore discuss this coupling. The stop-stop Higgs couplings, like the stop mass matrix, emerge essentially from the F-terms in the scalar potential (there is a residual D term component $\propto M_Z^2$). With the angle α in the Higgs mixing matrix, the $\tilde{t}_1\tilde{t}_1 h$ coupling is (we write the potential)

$$\begin{aligned} V_{\tilde{t}_1\tilde{t}_1 h} &= -g\frac{m_t}{M_W}\frac{\cos\alpha}{\sin\beta}\Big((A_t - \mu\tan\alpha)\sin\theta_{\tilde{t}}\ \cos\theta_{\tilde{t}}\ -\ m_t \\ &+ \frac{M_Z^2}{m_t}\frac{\sin\beta}{\cos\alpha}\sin(\alpha+\beta)\left((\frac{1}{2}-\frac{2}{3}\sin^2\theta_W)\cos^2\theta_{\tilde{t}} + \frac{2}{3}\sin^2\theta_W\sin^2\theta_{\tilde{t}}\right)\Big) \end{aligned} \tag{3.18}$$

The vertex does involve some important parameters which stem from the Higgs sector, notably the angle α. In the decoupling limit [17] which we are most interested in and up to radiative corrections Eq. 3.18 writes

$$
\begin{aligned}
V_{\tilde{t}_1\tilde{t}_1 h} &= +gR\frac{1}{M_W}\Big\{m_t^2+\sin\theta_{\tilde{t}}\,\cos\theta_{\tilde{t}}\left(\sin\theta_{\tilde{t}}\,\cos\theta_{\tilde{t}}(m_{\tilde{t}_1}^2-m_{\tilde{t}_2}^2)-\frac{m_t\,\mu\,r}{\tan\beta}\right)\\
&+ M_Z^2((2+r)\cos^2\beta-1)\left((\frac{1}{2}-\frac{2}{3}\sin^2\theta_W)\cos^2\theta_{\tilde{t}}+\frac{2}{3}\sin^2\theta_W\sin^2\theta_{\tilde{t}}\right)\Big\}
\end{aligned}
\tag{3.19}
$$

We see that in the limit $r \ll 1$ where r is neglected, the $\tilde{t}_1\tilde{t}_1 h$ very much simplifies. Note that neglecting the correction due to r, the coupling no longer depends on μ. Notice also that Eq. 3.19 shows that this correction is reduced as $\tan\beta$ gets larger. Discarding the r correction altogether, we end up with a compact formula

$$
\begin{aligned}
V_{\tilde{t}_1\tilde{t}_1 h} &\simeq \frac{g}{M_W}\Big(\sin^2(2\theta_{\tilde{t}})\frac{(m_{\tilde{t}_1}^2-m_{\tilde{t}_2}^2)}{4}+m_t^2\\
&+ M_Z^2\cos(2\beta)\left((\frac{1}{2}-\frac{2}{3}\sin^2\theta_W)\cos^2\theta_{\tilde{t}}+\frac{2}{3}\sin^2\theta_W\sin^2\theta_{\tilde{t}}\right)\Big)
\end{aligned}
\tag{3.20}
$$

We also confirm that the $\tan\beta$ dependence in the vertex is also hardly noticeable. Eq. 3.20 makes it clear that even for maximal mixing, $\sin^2 2\theta_{\tilde{t}} \sim 1$ the contribution of the stops and that of the top cancel each other thus leading to a very small vertex. The dip occurs for values of the mixing angle such that:

$$
\sin^2 2\theta_{\tilde{t}} \simeq \frac{4m_t^2}{m_{\tilde{t}_2}^2-m_{\tilde{t}_1}^2} \tag{3.21}
$$

On the other hand when the mixing is negligible, the vertex is accounted for almost entirely by the top mass and therefore has the same strength as the tth vertex.

The $\tilde{t}_2\tilde{t}_2 h$ vertex can be obtained from $\tilde{t}_1\tilde{t}_1 h$ by $\sin\theta_{\tilde{t}} \leftrightarrow \cos\theta_{\tilde{t}}$ and $m_{\tilde{t}_1} \leftrightarrow m_{\tilde{t}_2}$. Therefore if the $\tilde{t}_2\tilde{t}_2 h$ and $\tilde{t}_1\tilde{t}_1 h$ vertices were to be added, the mixing terms do not survive, as expected since the latter mix the left and right states. This is to be kept in mind. In situations where the stop masses are of the order of the top mass so that they both contribute to $h \to gg$ or $h \to \gamma\gamma$, the effect of mixing will, to a large extent, be washed away.

Already at this point we can attempt to predict the general features in $R_{gg\gamma\gamma}$ and $R_{\gamma\gamma}$ that will be introduced by large mixing in the stop sector. Consider the large M_A limit where the $\tilde{t}_1\tilde{t}_1 h$ vertex is most transparent, see Eq. 3.20. Naturally the stop will contribute if its mass is not too large and if its coupling to the Higgs is also large. When there is no mixing, only the diagonal m_t^2 term in Eq. 3.20 will, in both $\Gamma(h \to gg)$ and $\Gamma(h \to \gamma\gamma)$, interfere *constructively* with the top quark contribution. We therefore expect

an enhancement of $\Gamma(h \to gg)$, that is of the inclusive production. On the other hand, the fact that the top/stop loops and W interfere destructively, means that $\Gamma(h \to \gamma\gamma)$ will get smaller. Nonetheless since the W loop is much larger than the top loop, the reduction in the two-photon decay width will be modest compared to the enhancement in the two gluon width. Considering that at large M_A the width into $b\bar{b}$ (thus the total width) is hardly affected by mixing and hence sensibly the same as in the $\mathcal{SM}$, direct production $\sigma(pp \to h \to \gamma\gamma)$ is enhanced. At the same time associated Wh/Zh and $t\bar{t}h$ with the subsequent two-photon decay of the Higgs will be reduced somehow. For moderate mixing the $\tilde{t}_1\tilde{t}_1h$ vertex gets vanishingly small: here no effect is to be expected, either in any of the associated productions nor in the direct production. When the mixing gets very large so that now, it is the term in $m^2_{\tilde{t}_2}$ in Eq. 3.20 which dominates, the sign of the interferences between the stop and the top quark loop gets reversed. In this situation direct production can get extremely small, the stop loop cancelling the top loop. In the two photon decay, on the other hand when this cancellation takes place it still leaves the large W contribution. Nonetheless, the increase in $R_{\gamma\gamma}$ will be modest compared to the dramatic decrease in $R_{gg\gamma\gamma}$. Since the total width is hardly affected by these mixing effects the direct inclusive production will be much reduced. However associated Wh/Zh and $t\bar{t}h$ gets enhanced in these situations.

3.2 $pp \to \tilde{t}_1\tilde{t}_1^*h$ at the LHC

Because $\tilde{t}_1$ is relatively light and its coupling to the Higgs (h) large, associated stop cross sections can, exceptionally, be of the order of that of the associated top cross section[24] or even larger. At the LHC this cross section is essentially induced by gluon gluon fusion and is therefore directly proportional to the square of the $\tilde{t}_1\tilde{t}_1h$ vertex. We have recalculated this cross section with the help of a modified version of `CompHep`[36] to properly take into account the radiative corrections to the Higgs mass and couplings. For our analysis we have found it useful to calculate the cross section at the LHC by taking, as a reference point, the m_t^2 term only in the $\tilde{t}_1\tilde{t}_1h$ vertex, Eq. 3.20. The cross section can then be easily evaluated by specifying as independent input parameters $m_{\tilde{t}_1}$ and m_h only. The corresponding cross sections are shown in Fig. 4 and Fig. 5. We have made a polynomial fit, in the variables $m_h - m_{\tilde{t}_1}$ to these cross sections that reproduces the full results with a precision better than 2%, which is well within the uncertainty due to the choice of scale and structure function. Once a set of SUSY parameters is given, apart from the stop masses and $\tan\beta$ it will also furnish the corresponding Higgs mass, m_h, and the proper $\tilde{t}_1\tilde{t}_1h$ vertex can be evaluated. One can then properly normalise our cross sections. Considering the relative complexity of the $pp \to \tilde{t}_1\tilde{t}_1h$ cross section this method is much more efficient when we are scanning over many SUSY parameters as done in the present

analysis since we do not have to recalculate the $pp \to \tilde{t}_1\tilde{t}_1 h$ for each scan. Our results agree with those shown in [24] as well as in [37], however the largest cross sections shown in [24] do not pass our constraint on the Higgs mass $m_h > 90$GeV and/or $\Delta\rho$ (see below).

3.3 The $\tilde{t}_2\tilde{t}_1 h, A, H$ vertex and $\tilde{t}_2 \to \tilde{t}_1 h, H, A$

The $\tilde{t}_1\tilde{t}_2 h$ vertex may be cast into

$$\begin{aligned} V_{\tilde{t}_1\tilde{t}_2 h} &= +gR\frac{1}{M_W}\Big\{\frac{\cos 2\theta_{\tilde{t}}}{4}\left(\sin 2\theta_{\tilde{t}}\,(m^2_{\tilde{t}_1} - m^2_{\tilde{t}_2}) - \frac{2m_t\,\mu\,r}{\tan\beta}\right) \\ &+ M_Z^2 \sin 2\theta_{\tilde{t}}\,(\cos 2\beta + r\cos^2\beta)\left(\frac{2}{3}\sin^2\theta_W - \frac{1}{4}\right)\Big\} \\ &\to +gR\frac{1}{4M_W}\sin 4\theta_{\tilde{t}}\,(m^2_{\tilde{t}_1} - m^2_{\tilde{t}_2}) \end{aligned} \tag{3.22}$$

It is crucial to note that within the approximation of neglecting the r terms and the D-terms, this coupling does not survive in the maximal mixing scenario, it is proportional to $\sin(4\theta_{\tilde{t}})$. Nonetheless because of it its Yukawa nature this can be a rather large coupling and therefore phase-space allowing $Br(\tilde{t}_2 \to \tilde{t}_1 h)$ can be large. Considering that $\tilde{t}_2$ pair production exceeds 1pb for $m_{\tilde{t}_2} \leq 500$GeV (See Fig. 6), $\tilde{t}_2$ can trigger Higgs (h) production[7].

Contrary to $\chi_2^0 \to \chi_1^0 h$ whose branching ratio can reach 100% for some of the SUSY parameters[15] and thus very efficiently triggers Higgs production, $Br(\tilde{t}_2 \to \tilde{t}_1 h)$[16] can never reach 100%. This is because, independently of other decay modes into the $b, \tilde{b}$ sector, there is always the competing larger decay rate $\tilde{t}_2 \to \tilde{t}_1 Z$. Indeed when the splitting is large $\tilde{t}_2 \to \tilde{t}_1 Z$ can be approximated by $\tilde{t}_2 \to \tilde{t}_1\phi^0$, ϕ^0 being the neutral Goldstone Boson, with an effective coupling $g\frac{1}{4M_W}\sin 2\theta_{\tilde{t}}\,(m^2_{\tilde{t}_2} - m^2_{\tilde{t}_1}) = g/2M_W m_t(A_t + \mu/\tan\beta)$.

When M_A is small, $\tilde{t}_2$ can also provide a welcome source of pseudo-scalar (and heavy Higgses) through $\tilde{t}_2 \to \tilde{t}_1 A, H$. What's more, the strength of the $\tilde{t}_2 \to \tilde{t}_1 A$ coupling does not depend on the stop mixing angle:

$$V_{\tilde{t}_1\tilde{t}_2 A} = ig\frac{m_t}{2M_W}\left(\frac{A_t}{\tan\beta} - \mu\right) \tag{3.23}$$

The decay $\tilde{t}_2 \to \tilde{t}_1 H$ is generally smaller and vanishes when the mixing is maximal. In the decoupling limit this becomes:

$$V_{\tilde{t}_1\tilde{t}_2 H} \sim ig\cos 2\theta_{\tilde{t}}\frac{m_t}{2M_W}\left(\frac{A_t}{\tan\beta} - \mu\right) \tag{3.24}$$

[7] $\tilde{t}_1\tilde{t}_2$ is completely negligible at the LHC[39].

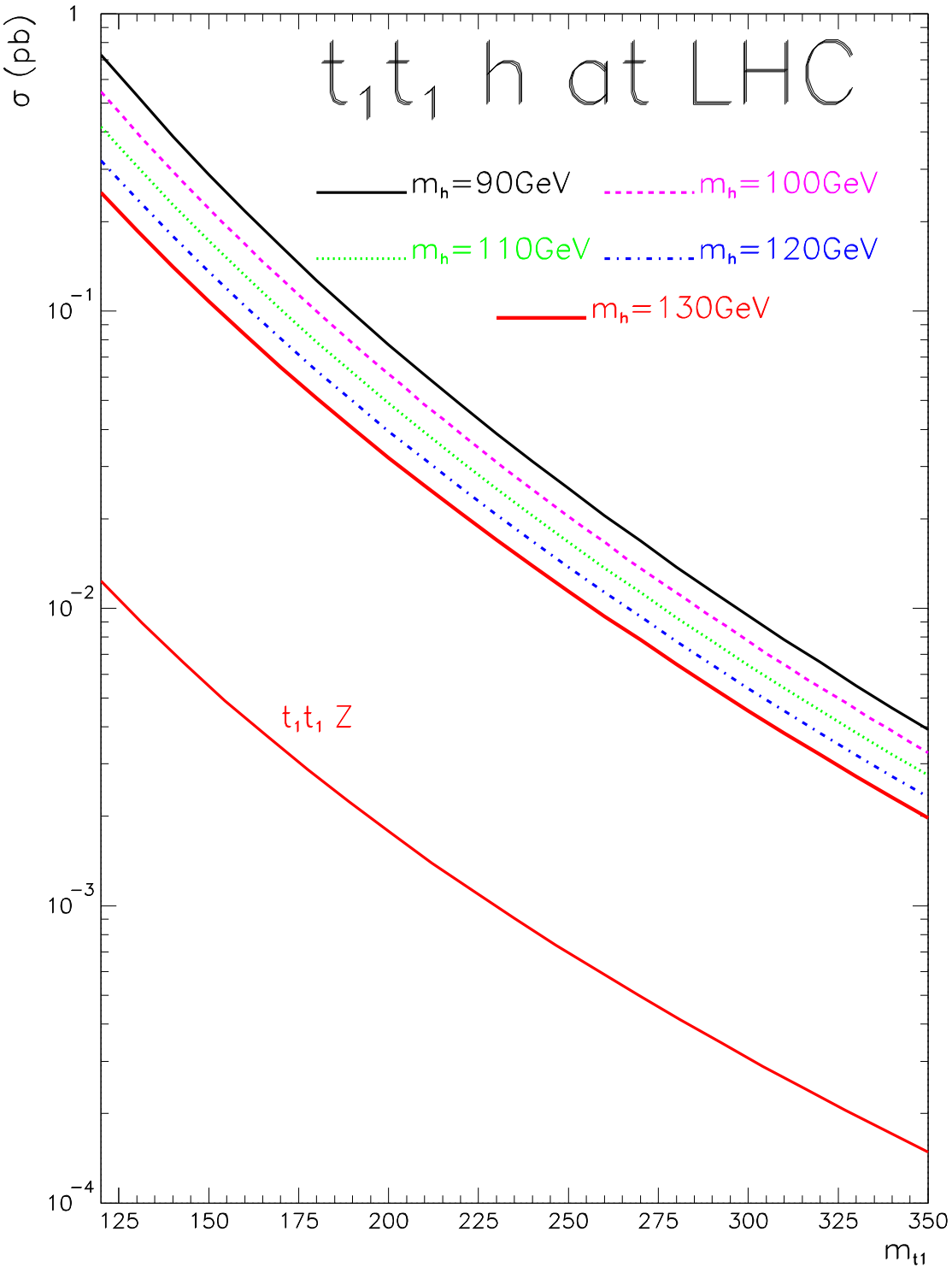

Figure 4: $\tilde{t}_1\tilde{t}_1 h$ *at the LHC as a function of* $m_{\tilde{t}_1}$ *and for a range of SUSY Higgs masses. The* $\tilde{t}_1\tilde{t}_1 h$ *vertex is set in the limit of large* M_A *with no mixing and no D-term, see text of how to normalise it when the SUSY parameters are fixed. Also shown is* $\tilde{t}_1\tilde{t}_1 Z$*. For the latter the vertex has been computed with* $\cos^2\theta_{\tilde{t}} = 1/2$*, i.e. maximal mixing. For other values of the mixing, rescale by using the vertex* $(\cos^2\theta_{\tilde{t}}/2 - 2/3 s_W^2)$*. We have taken the CTEQ4 structure function with a scale set at the invariant mass of the subprocess.*

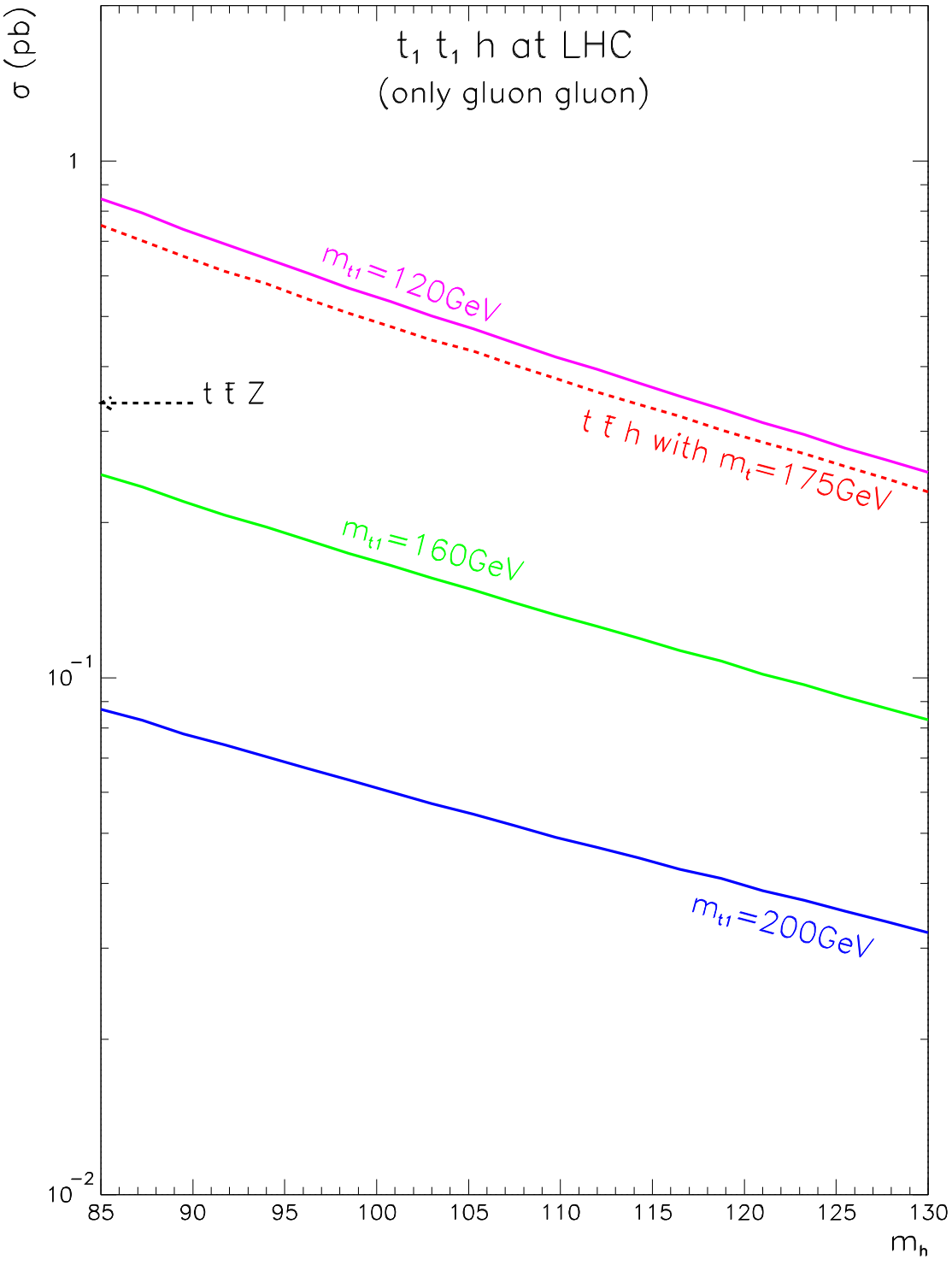

Figure 5: *As in Figure 4 but as function of the Higgs mass. The $t\bar{t}h$ is also shown for comparison for the same set of structure functions and by only taking into account the gluon gluon processes. For the latter including the small quark initiated process, our results agree with [38]. Also shown is $t\bar{t}Z$.*

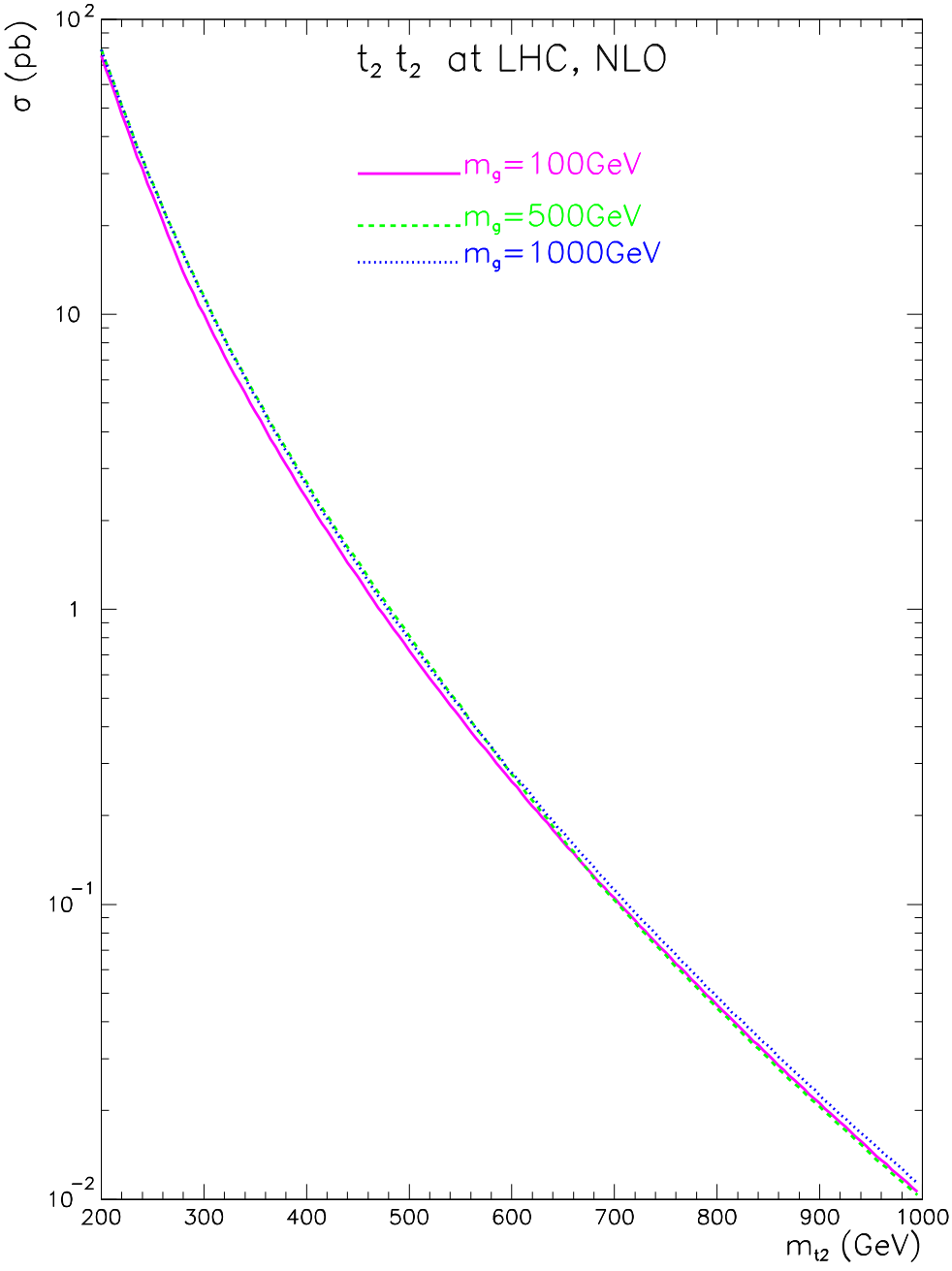

Figure 6: *Next-to-leading order $\tilde{t}_1$ pair production at the LHC, for three representative values of the gluino mass. We used the code given to us by Michael Spira[39].*

Of course to calculate the branching ratios of $\tilde{t}_2$ into Higgses we have evaluated all possible widths of $\tilde{t}_2$, without QCD corrections though. We have checked our numbers against those of [40] as well as the output of `GRACE` [41]. For a general recent review of stop decays see [35, 42]. For further reference note that whenever stop mixing is not excessively small, we can reach $Br(\tilde{t}_2 \to \tilde{t}_1 h) \sim 10\%$. Associated $\tilde{t}_2\tilde{t}_1 A$ in mSUGRA has also been entertained recently[37]. However in the mSUGRA scenario the mixing is generally not large and the stops are usually heavy leading to small cross section for Higgs production through stops. But then in this same scenario large drops in the inclusive production due to stop mixing hardly occur either.

3.4 Constraints from low Higgs masses, $\Delta\rho$ and CCB

Large values of the $\tilde{t}_1\tilde{t}_1 h$ vertex which lead to the largest $pp \to \tilde{t}_1\tilde{t}_1 h$ and the sharpest drop in $R_{gg\gamma\gamma}$ occur when the mixing is large with a large splitting between the two stop physical masses. It is, however, for this configuration that one has some strong constraints which preclude the highest values of the cross section. For instance, one has to be wary that imposing a lower bound on the Higgs mass, from its non observation at LEP2 say, can restrict drastically the $\sin 2\theta_{\tilde{t}} - m_{\tilde{t}_2}$ parameter space. This constraint is very much dependent on $\tan\beta$. Much less dependent on $\tan\beta$ but a quite powerful one, for the values of $m_{\tilde{t}_1}$ that we have entertained, is the constraint coming from $\Delta\rho$[43]. Taking the present limit $\Delta\rho < .0013$ applicable to New Physics with a light Higgs[44], which here means essentially the contribution from stops and sbottoms (and marginally the Higgs sector[8]) generally excludes region of the parameter space where the $\tilde{t}_1\tilde{t}_1 h$ is largest. In our $\Delta\rho$ constraint we have relied on the two-loop calculation of [45], which can enhance $\Delta\rho$ by as much as 10% even with a heavy gluino.

One more constraint one needs to mention. In the stop sector and in the presence of large mixing as is the case here, one often has to check whether the parameters do not induce colour and charge breaking global minima (CCB)[46]. It has been argued that the constraints based on the global minima may be too restrictive[47]. It was shown that for a wide range of parameters, the global CCB minimum becomes irrelevant on the ground that the time required to reach the lowest energy state exceeds the present age of the universe. Taking the tunneling rate into account results in a milder constraint which may be approximated[47] by :

$$A_t^2 + 3\mu^2 < 7.5(M_{\tilde{Q}_3}^2 + M_{\tilde{t}_R}^2) \tag{3.25}$$

[8]For light stops in the decoupling limit the sbottom-stop contribution when substantial gives a positive contribution, whereas the Higgs sector contributes a negligible negative contribution.

When presenting our results we will, unless otherwise stated, impose the limits $m_h > 90\text{GeV}$, $\Delta\rho < .0013$ together with the mild CCB constraint Eq. 3.25. Considering that the CCB constraint is rather uncertain, it is worth pointing out that our CCB constraint hardly precludes points which are not already rejected by $\Delta\rho$ and m_h.

Apart from the indirect constraints we also imposed, the model independent limit, $m_{\tilde{t}_1}, m_{\tilde{b}_1} > 80\text{GeV}$ from present direct searches[48]. Our limit on the stop, is however superseded by our constraint that the lightest neutralino is the LSP and that $\tilde{t}_1 \to c\chi_1^0$[49] is always open. When taking $\mu = -M_2 = 250\text{GeV}$ with the unification condition, $\chi_1^0 \simeq 120\text{GeV}$ and thus $m_{\tilde{t}_1} > 120\text{GeV}$.

3.5 $\tan\beta = 2.5$

We start our analysis by considering the case with $\tan\beta = 2.5$. Although this value is not far from being excluded by the direct LEP2 searches[1], depending on the exact SUSY parameters, we study it here in order to compare our results with those in[9] and to show a feature which is not present for higher values of $\tan\beta$.

3.5.1 The case of a common mass in the third generation squark sector

We first revisit the case[7, 9] of allowing, at the electroweak scale, a common mass for all the supersymmetric masses of the third generation squarks: $\tilde{m}_{\tilde{Q}_3} = \tilde{m}_{\tilde{U}_{3R}} = \tilde{m}_{\tilde{D}_{3R}} = \tilde{m}_{\tilde{3}}$. Taking a common value for the SU(2) and U(1) masses shows that unless the effective tri-linear term is negligible, $\tilde{A}_t \sim 0$, this leads to $|\sin 2\theta_{\tilde{t}}| = 1$, see Eq. 3.16. We note that contrary to what is claimed in[9] this situation, although common for the first two generation of squarks, occurs only in exceptional situations in a model such as mSUGRA. Moreover in mSUGRA A_t is controlled almost entirely by $m_{1/2}$, the common gaugino mass, and thus would not be excessively large[50]. Leaving this aside, this assumption helps keep the number of parameters to a minimum while concentrating on the impact of mixing. To that effect we have set, apart from the common third family scalar quark $\tilde{m}_{\tilde{3}}$ which was allowed to vary in the range $100 - 1000\text{GeV}$ and $M_A = 1\text{TeV}$, all other sfermion masses to 500GeV. Moreover we have assumed the unification condition for the gaugino masses and set the Higgsino mass $M_2 = -\mu = 250\text{GeV}$. We then scanned over A_t, $-1000 \leq A_t/(GeV) \leq 1000$ and $\tilde{m}_{\tilde{3}}$. Note that since we are scanning over both positive and negative values of A_t, some important mixing effects sensitive to the sign of $A_t \times \mu$ are covered even though we have fixed the sign of μ. Among the 2.10^4 generated point for each $\tan\beta$ half passed all the constraints.

First as shown in Fig. 7, we do confirm that the reduction in the two-photon signal

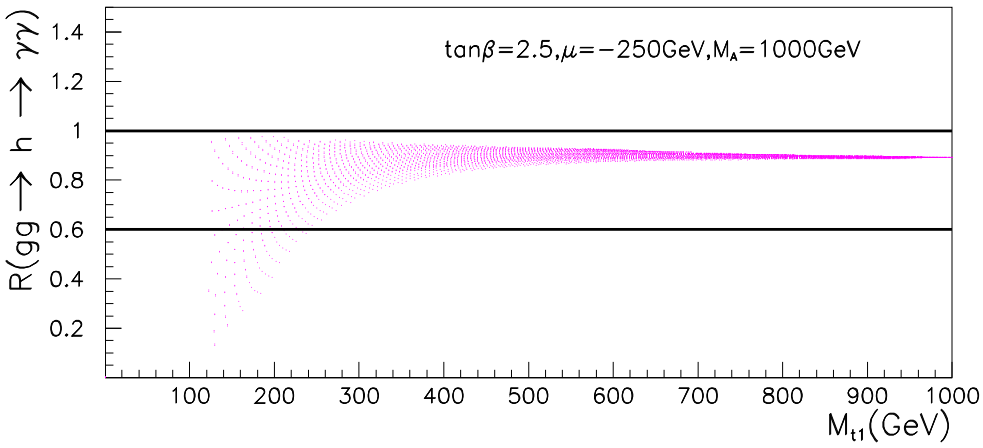

Figure 7: $R_{gg\gamma\gamma}$ *vs* $m_{\tilde{t}_1}$ *for* $\tan\beta = 2.5, \mu = -250\,GeV$ *and* $M_A = 1\,TeV$.

in the direct channel is most dramatic for the lowest values of the stop mass, although a low stop mass does not always mean that a reduction has to occur. As a matter of fact there are more points that generates a low $m_{\tilde{t}_1}$ and give $R_{gg\gamma\gamma} \geq .6$, say, than those that give $R_{gg\gamma\gamma} \leq .6$. Note that most points clustering around values corresponding to little mixing or large stop masses. Therefore the very rare situations corresponding to very sharp drops could be interpreted as at best unnatural. It is also worth pointing out that values such that $R_{gg\gamma\gamma} \geq 1.$ are not obtained for $\tan\beta = 2.5$. We have verified that while, in principle, this was possible for $\tan\beta = 2.5$ this possibility was ruled out by the requirement of having $m_h \geq 90$GeV.

As stressed numerous times, for the intermediate mass Higgs in the direct channel decaying into two photons, the significance depends crucially on the Higgs mass. It is therefore important to localise for which values of the Higgs mass, the reductions are most drastic. For $\tan\beta = 2.5$ we see, Fig. 8, that this reduction gets worse, $R_{gg\gamma\gamma} \simeq .2$ for Higgs masses clustered around ~ 103GeV.

It is important to note, on the other hand, that for Higgs masses around 90GeV where the ($\mathcal{SM}$) Higgs signal is most difficult to extract, the effect of the stop is rather negligible (here there is no mixing hence the low mass of the Higgs which does not get further radiative corrections). Therefore this is a welcome point. As compared to the case of CLASS-H with $M_A = 180$GeV and $\tan\beta = 2.5$, for which $M_h = 90$GeV, $R_{gg\gamma\gamma}$ reaches .3 whereas for the same Higgs mass (and $\tan\beta$) our points cluster around one. An even

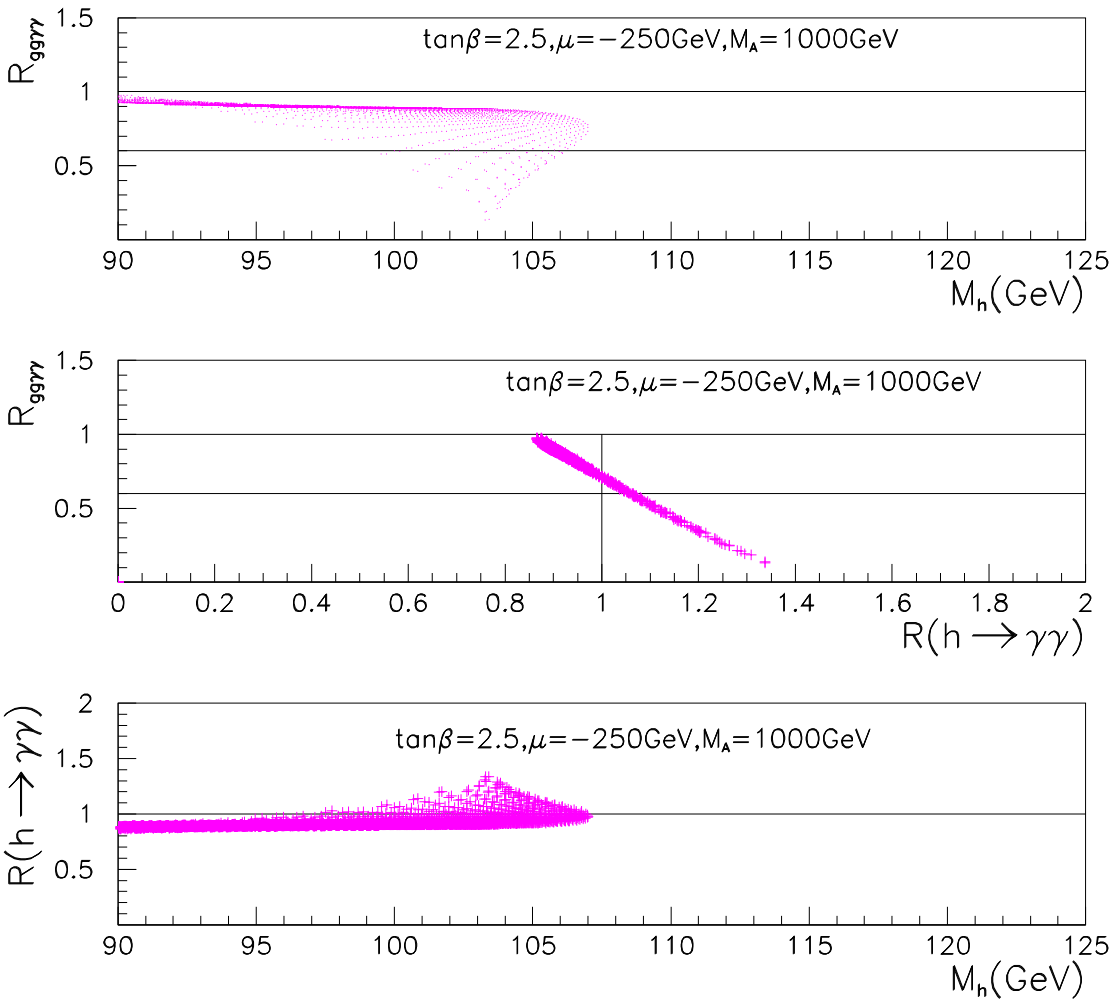

Figure 8: *As in Fig. 7 but for a)* $R_{gg\gamma\gamma}$ *vs* M_h*, b)* $R_{gg\gamma\gamma}$ *vs* $R_{\gamma\gamma}$ *and c)* $R_{\gamma\gamma}$ *vs* M_h*.*

more important remark concerns the behaviour of the branching ratio into two photons. We find, see Fig. 8, that the branching ratio into photons in this SUSY scenario increases at the same time as the direct production decreases, in sharp contrast to what happens in CLASS-H when M_A decreases. This confirms our expectations. The $R_{gg\gamma\gamma}$ *vs* $R_{\gamma\gamma}$ can be considered as a signature of this scenario. In the corresponding scatter plot of Fig. 8, the points fall almost along a line and shows that when $R_{gg\gamma\gamma} \leq .8$, $R_{\gamma\gamma} \geq 1$. Considering that in this large M_A scenario and even in the presence of large mixing the $t\bar{t}h$ and Wh are sensibly the same as in the standard model, the associated Higgs production with the Higgs decaying into two-photon should pose no problem with the high luminosity LHC. We do not show the ratios for $t\bar{t}\gamma\gamma$ and $W\gamma\gamma$ as these are given essentially by the ratio $R_{\gamma\gamma}$, see Fig. 8 . To conclude, for this value of $\tan\beta = 2.5$, when $90 \leq m_h \leq 100$ observability of the lightest SUSY Higgs (h) is quite similar to that of the $\mathcal{SM}$. Above these values, if the direct production is not possible, the branching into photons is larger than the $\mathcal{SM}$ and thus associated production provides more chance of detecting the Higgs. For instance, taking the $\mathcal{SM}$ Higgs CMS analysis[13] with a luminosity of 100fb^{-1} as a guide, shows that it is only in the range $100 - 105$ where values below .6 are possible for $R_{gg\gamma\gamma}$ that the Higgs may not be observed in the direct channel. The same analysis shows, however, that with the values that we obtain in the associated channels that there is no problem of cornering the Higgs. Note that for the most critical drop in the direct channel we have obtained a enhancement factor of up to 1.35 in the associated production. For such values even the ATLAS simulation[22, 12] with a luminosity of 100fb^{-1} indicates observation in the associated channels.

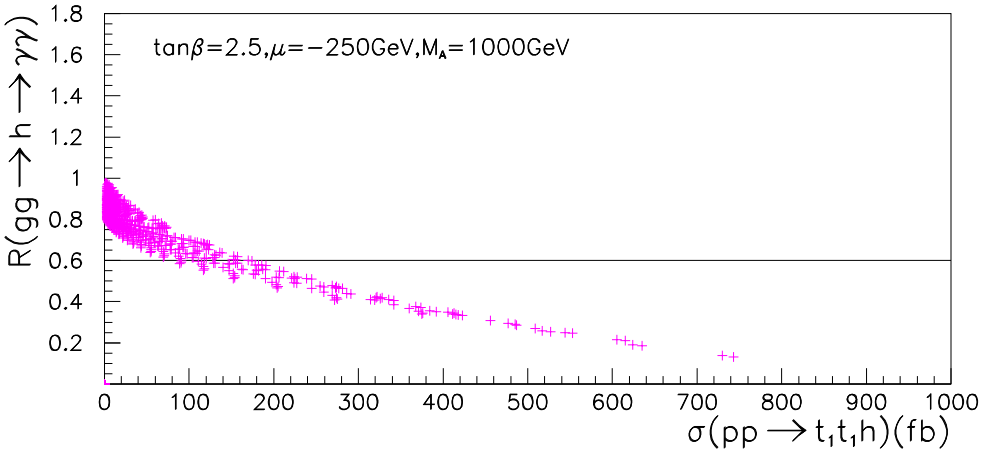

Figure 9: *As in Fig. 7 but for* $R_{gg\gamma\gamma}$ *vs* $\sigma(\tilde{t}_1\tilde{t}_1 h)(fb)$.

Finally, another note of optimism in the case where the drop in the inclusive production is severe is that production of h in association with stops could help also. As shown in Fig. 9, whenever $R_{gg\gamma\gamma} \leq .6$, $\sigma(\tilde{t}_1\tilde{t}_1 h)$ is in excess of 100fb and can reach as much as ~ 740fb. As a comparison, for these extreme cases for which $m_h \sim 100 - 105$GeV, one has $\sigma(t\bar{t}h) \simeq 500$fb. Considering that, see Fig. 7, these helpful $\tilde{t}_1\tilde{t}_1^* h$ cross sections are for values of $m_{\tilde{t}_1} \leq 250$GeV for which $R_{gg\gamma\gamma} \leq .6$, $\tilde{t}_1$ with our choice of parameters will decay exclusively into $c\chi_1^0$. It remains to be seen whether this constitutes a viable signal and whether we could use the Higgs decays into $b\bar{b}$, which by the way is not much affected at these low values $\tan\beta$ by these mixing effects. The signal would be $b\bar{b} + \text{jets} + \not{p}_T$. Note that the continuum $\tilde{t}_1\tilde{t}_1 Z$ is quite small. For $m_{\tilde{t}_1} = 120$GeV and maximal stop mixing angle, after folding with $Br(Z \to b\bar{b})$ the continuum leads to a dismal raw cross section of about 1fb.

3.5.2 Lifting the degeneracy in the third family scalar masses

We have already argued that the scenario with exactly equal squark masses for the third generation is very special and even unnatural. Taking a more general framework, we move away from the case of maximal mixing. As we have discussed this can open up new possibilities, notably $\tilde{t}_2 \to \tilde{t}_1 h$ decays. For illustration, we have taken $\tilde{m}_{\tilde{t}_{3R}} = 200$GeV, $\tilde{m}_{\tilde{b}_{3R}} = 500$GeV and allowed $50 \leq \tilde{m}_{\tilde{Q}_3} \leq 500$GeV. In order to compensate for the deviation from maximal mixing, the trilinear coupling was allowed to vary in the range $-2000 \leq A_t \leq 2000$GeV. However very few points with $|A_t| \geq 1200$ pass our constraints, essentially from $\Delta\rho$. As expected the general features found in the case of maximal mixing are still present here, even though with our parameters the drops are not as dramatic as in the maximal mixing case. Another observation is that $m_h > 105$GeV is not generated. This is because contrary to the previous case the stop masses do not extend to 1TeV and hence the radiative corrections to the Higgs mass are not optimal. Nonetheless as seen in Fig. 10 a ratio $R_{gg\gamma\gamma}$ as low as .4 is possible and occurs for low $\tilde{t}_1$ masses. Again this drop occurs for a small range of Higgs masses sensibly the same as in the maximal mixing case, $m_h \sim 103 - 104$GeV, Fig. 10. However when this occurs one is saved by the fact that the branching ratio into photons is larger than in the $\mathcal{SM}$, Fig. 11. Moreover we still find that when $R_{gg\gamma\gamma}$ gets too small $pp \to \tilde{t}_1\tilde{t}_1^* h$ is of the order 100fb reaching a maximum of 200fb when $R_{gg\gamma\gamma}$ is lowest, Fig. 12. The main novelty here is $pp \to \tilde{t}_2\tilde{t}_2^* \to \tilde{t}_2\tilde{t}_1^* h$, with $Br(\tilde{t}_2 \to \tilde{t}_1 h) = \mathcal{O}(10\%)$. Because this stems from a two-body cross section, it can lead to quite large $\sigma(\tilde{t}_2\tilde{t}_1^* h)$ reaching as much 600fb, and therefore in many instances larger than the continuum $\tilde{t}_1\tilde{t}_1^* h$, Fig. 12. What is also worth noting is that these large cross sections do not necessarily occur when one has large drops in the inclusive two-photon channel. Moreover the signature in this channel should be cleaner, taking advantage of the cascade

decays of the other $\tilde{t}_2$ starting with $\tilde{t}_1 Z, \tilde{b}_1 W, b\tilde{\chi}^+_{1,2}, ...$ Of course there are points where neither $\tilde{t}_2\tilde{t}_1 h$[9] nor $\tilde{t}_1\tilde{t}_1 h$ exceeds 10fb,Fig. 12. However in this case the reduction in $R_{gg\gamma\gamma}$ is quite modest.

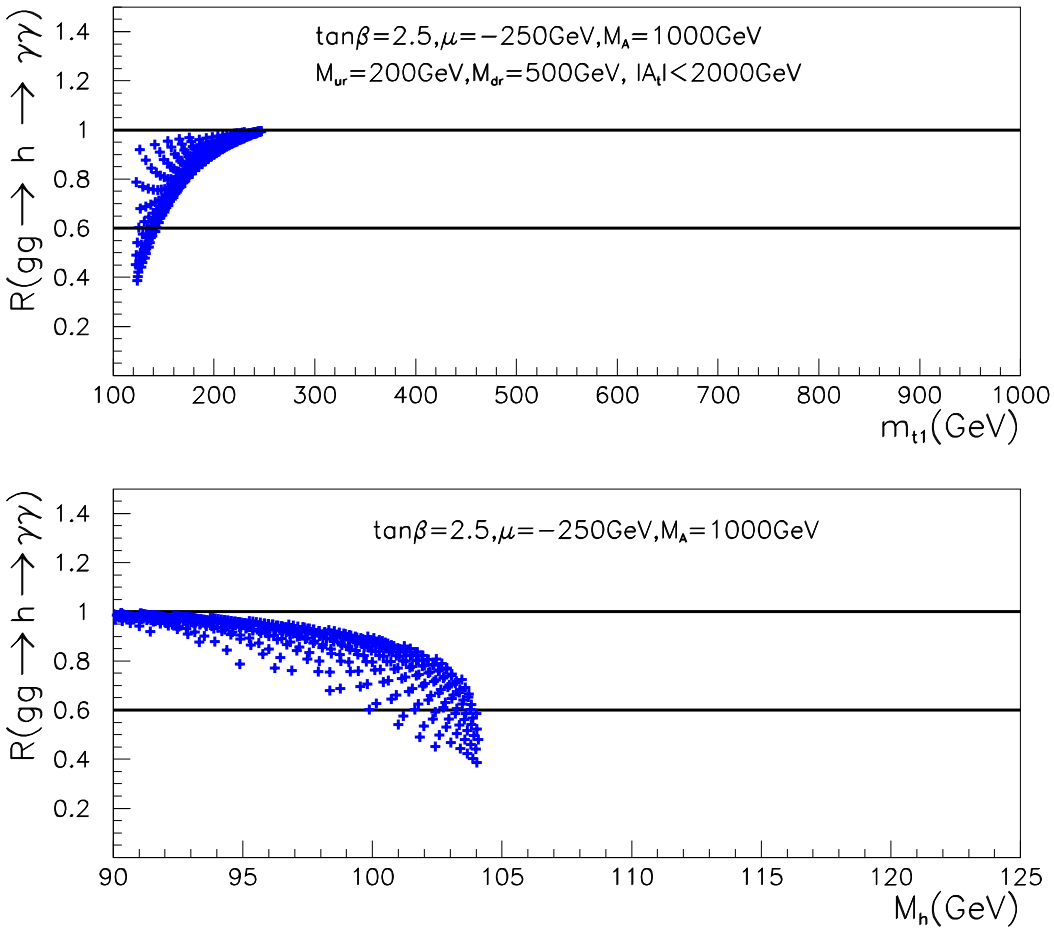

Figure 10: *a)* $R_{gg\gamma\gamma}$ *vs* $m_{\tilde{t}_1}$ *for* $\tan\beta = 2.5, \mu = -250 GeV$ *and* $M_A = 1 TeV$, *when we allow different scalar masses for the third generation as given, see text . b) As in a) but for* $R_{gg\gamma\gamma}$ *vs* M_h.

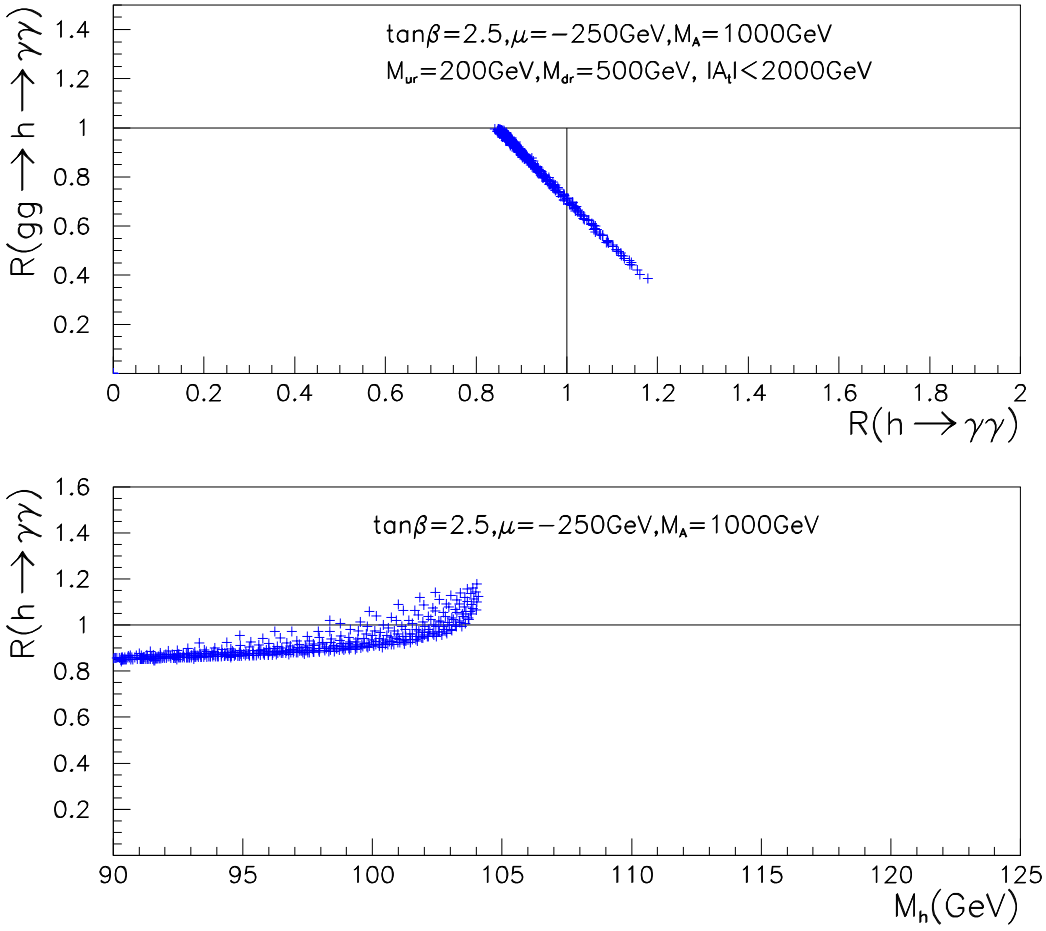

Figure 11: *As in Fig. 10 but for* $R_{gg\gamma\gamma}$ *vs* $R_{\gamma\gamma}$ *and* $R_{\gamma\gamma}$ *vs* M_h .

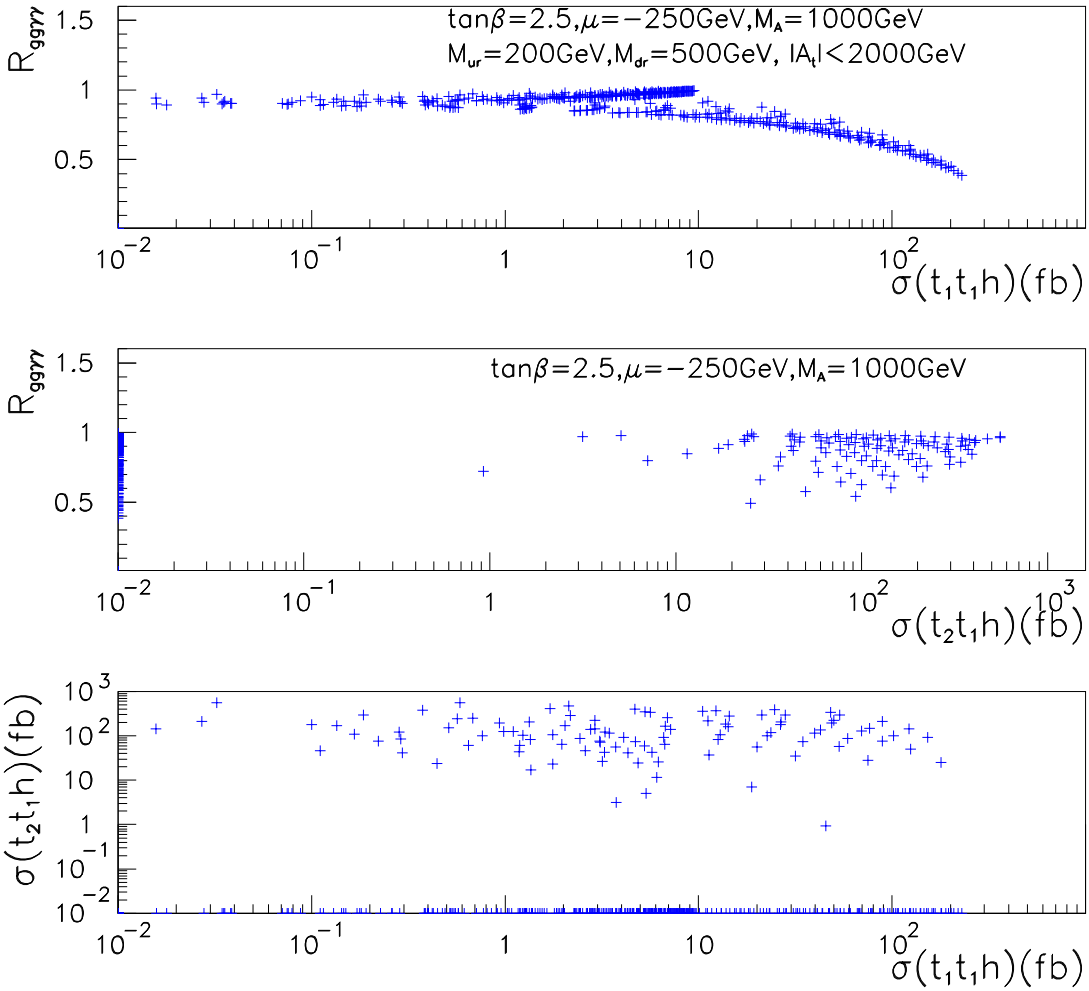

Figure 12: *As in Fig. 10 but for a)* $R_{gg\gamma\gamma}$ *vs* $\sigma(pp \to \tilde{t}_1\tilde{t}_1 h)$*, b)* $R_{gg\gamma\gamma}$ *vs* $\sigma(pp \to \tilde{t}_2\tilde{t}_1 h)$ *and c)* $\sigma(pp \to \tilde{t}_1\tilde{t}_1 h)$ *vs* $\sigma(pp \to \tilde{t}_2\tilde{t}_1 h)$*.* $\sigma(pp \to \tilde{t}_2\tilde{t}_1 h) \equiv \sigma(pp \to \tilde{t}_2\tilde{t}_1^* h + \tilde{t}_2^*\tilde{t}_1 h)$

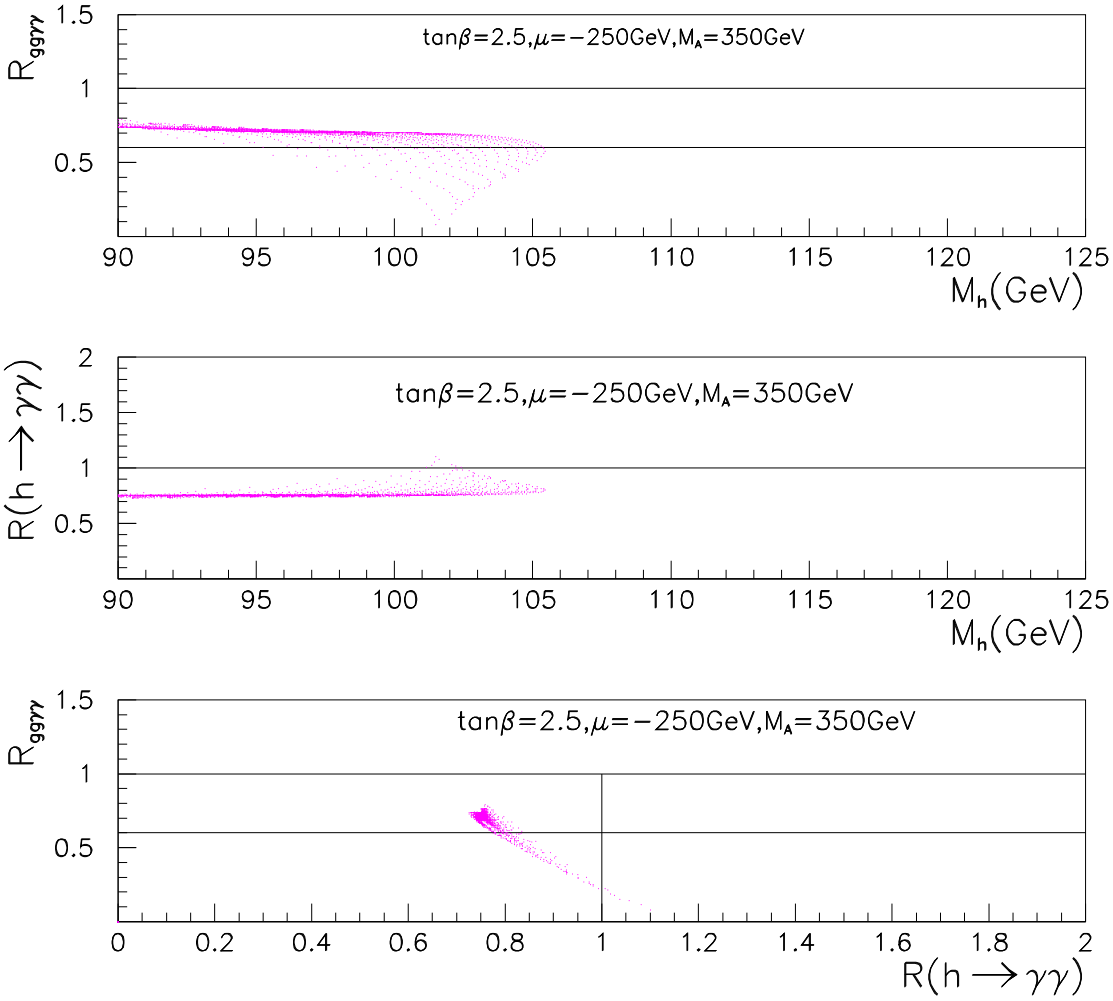

Figure 13: a) $R_{gg\gamma\gamma}$ *vs* M_h for $\tan\beta = 2.5, \mu = -250\text{GeV}$ and $M_A = 350\text{GeV}$, with equal squark masses. b) As in a) but for $R_{\gamma\gamma}$ *vs* M_h. c) As in a) but for $R_{gg\gamma\gamma}$ *vs* $R_{\gamma\gamma}$.

3.5.3 Stop mixing with a low M_A

We have seen in section 2, in the case of no-mixing, that as M_A decreases both the inclusive and associated two-photon channels decrease, mainly because of an increase in the width into $b\bar{b}$ which dominates the total width and hence reduces the two-photon branching ratio. Since $hb\bar{b}$ is hardly affected by the mixing effect, this decrease due to M_A will also be present in the case of mixing and hence reduces the significance of the two-photon channel. This overall reduction, independent of mixing, can be evaluated by using Eq. 2.10. Likewise since the $\tilde{t}_1\tilde{t}_1h$ vertex carries the same reduction R as the $t\bar{t}h$ vertex, see Eq. 3.19, an overall M_A- reduction in $R_{gg\gamma\gamma}$, which can be approximated by Eq. 2.11, will take effect beside the pure large stop mixing effects that we have discussed in the $M_A = 1$TeV limit. We first consider the case of a moderate $M_A = 350$GeV with all other masses as in section 3.5.1. Figs. 13 show that those points for which at large M_A the effect of mixing were most drastic on $R_{gg\gamma\gamma}$ are not much further reduced. They occur for masses which are sensibly the same as with the much larger M_A. Note however that the optimal values of $R_{gg\gamma\gamma}$ are reduced from about 1 to .8 and occur also for $M_h \sim 90$GeV. This reduction is essentially what we would have obtained by applying the factor $R_{gg\gamma\gamma}$ calculated using Eq. 2.11. For this value of M_h now detectability may be a problem if the luminosity is low, especially that the corresponding $R_{\gamma\gamma}$ is about .75, which may also preclude detection in the associated Higgs production, Figs. 13. With these values occuring at such low values of m_h, even CMS[13] with $30fb^{-1}$ will miss the Higgs, but again there should be no problem in the associated production after collecting $\sim 100fb^{-1}$. Still, whenever mixing becomes important and reduces $R_{gg\gamma\gamma}$ significantly, associated production should be no problem. For instance when $R_{gg\gamma\gamma}$ is below .4, $R_{\gamma\gamma} \geq .95$. In these configurations $Br(h \to \gamma\gamma)$ benefits from the increase in $\Gamma(h \to \gamma\gamma)$ which is not completely offset by the increase in $\Gamma(h \to b\bar{b})$. In these configurations with small $\tilde{t}_1$, $\tilde{t}_1\tilde{t}_1h$ could help with $\sigma(\tilde{t}_1\tilde{t}_1h) = 100 - 780$fb, Fig. 14.

We may argue that had we taken a much lower value of M_A we would have introduced a larger reduction in $R_{\gamma\gamma}$ which may affect dangerously the associated production. We would then be in a situation where the inclusive cross section is down because of large mixing in the stops and the associated production small mainly because the branching into photons is down as a result of M_A being low. Note however that in these situations we would be far from the decoupling regime, with all Higgses being relatively light and a very light stop having large couplings to the Higgses. One consequence of this light spectrum is that, even in the case of maximal stop mixing where $\tilde{t}_2 \to \tilde{t}_1h$ is inhibited,

[9] With our set of parameters one would expect that some points with maximal mixing are generated. However we have checked that these do not pass all the constraints. This explains why we never get a vanishingly small $\tilde{t}_2\tilde{t}_1h$ cross section.

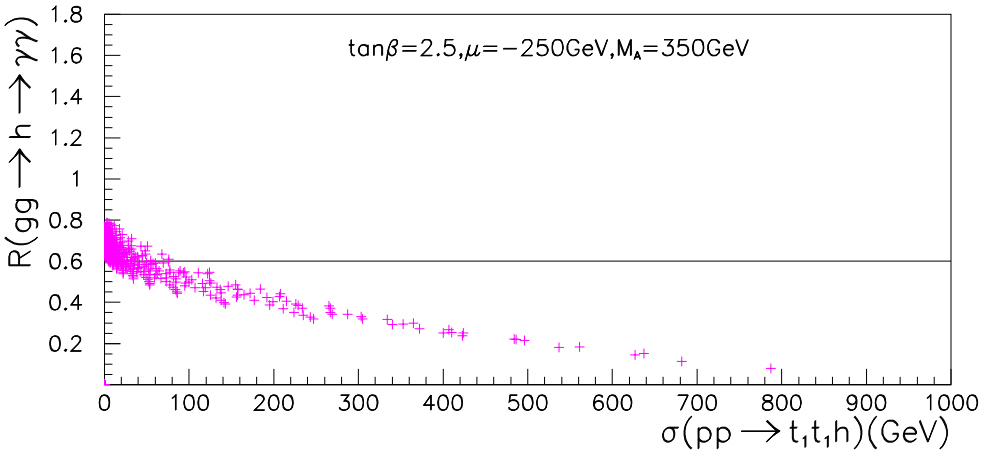

Figure 14: *As in Fig. 13 but for* $R_{gg\gamma\gamma}$ *vs* $\sigma(pp \to \tilde{t}_1\tilde{t}_1 h)$.

the $\tilde{t}_1\tilde{t}_2 A$ coupling is large, Eq. 3.23 and can be such that it triggers $\tilde{t}_2 \to \tilde{t}_1 A$. This is because large mixing and large splitting between the stop, allows enough phase space for a relatively light pseudo-scalar. To illustrate this fact, we have lowered M_A to 250GeV. The gross features found for $M_A = 350$GeV are still present as concerns the inclusive production of h Fig. 15, with an overall reduction factor due to $Br(h \to \gamma\gamma)$ which is slightly larger. At the same time the location of the drops are shifted to slightly lower values of m_h, which is a direct consequence of a low M_A. However as shown in Fig. 16, $\sigma(\tilde{t}_2\tilde{t}_1 A)$ can be quite large and often exceeds $\tilde{t}_1\tilde{t}_1 h$. Note that $\sigma(\tilde{t}_2\tilde{t}_1^* A)$ may be large even for points where the inclusive two-photon cross section is lowest, whereas $\tilde{t}_2\tilde{t}_1^* h$ is largest for regions where the inclusive cross section is most affected. Therefore we see that combining different channels in this scenario offers much better prospects than in the no-mixing case with the same low value of M_A. To start with, when the direct production is very much reduced, associated production has a better siginificance in the case of very large stop mixing compared to the no mixing case for the same M_A. Another interesting point is that although the main decay of A will be into $b\bar{b}$, we also find that $A \to Zh$ can be substantial. For instance, the chain $\sigma(pp \to \tilde{t}_2\tilde{t}_2 \to \tilde{t}_2\tilde{t}_1 A \to \tilde{t}_2\tilde{t}_1 Zh)$ can reach as much as 350fb (for this point $m_{\tilde{t}_1} = 129$GeV, $m_{\tilde{t}_2} = 396$GeV). For larger values of the stop masses ($m_{\tilde{t}_1} = 235$GeV, $m_{\tilde{t}_2} = 525$GeV), the same chain corresponds to 43fb. The decay $\tilde{t}_2 \to \tilde{t}_1 H$ is also possible, but the corresponding cross section, $\sigma(\tilde{t}_2\tilde{t}_1^* H)$ is below 10fb. This is because the branching ratio into H is about a factor $\cos^2 2\theta_{\tilde{t}}$ down compared to the branching ratio into A, while H and A are almost degenerate in mass, Eqs. 3.24- 3.23. To end this section let us mention that when the mass of the pseudo-scalar gets small,

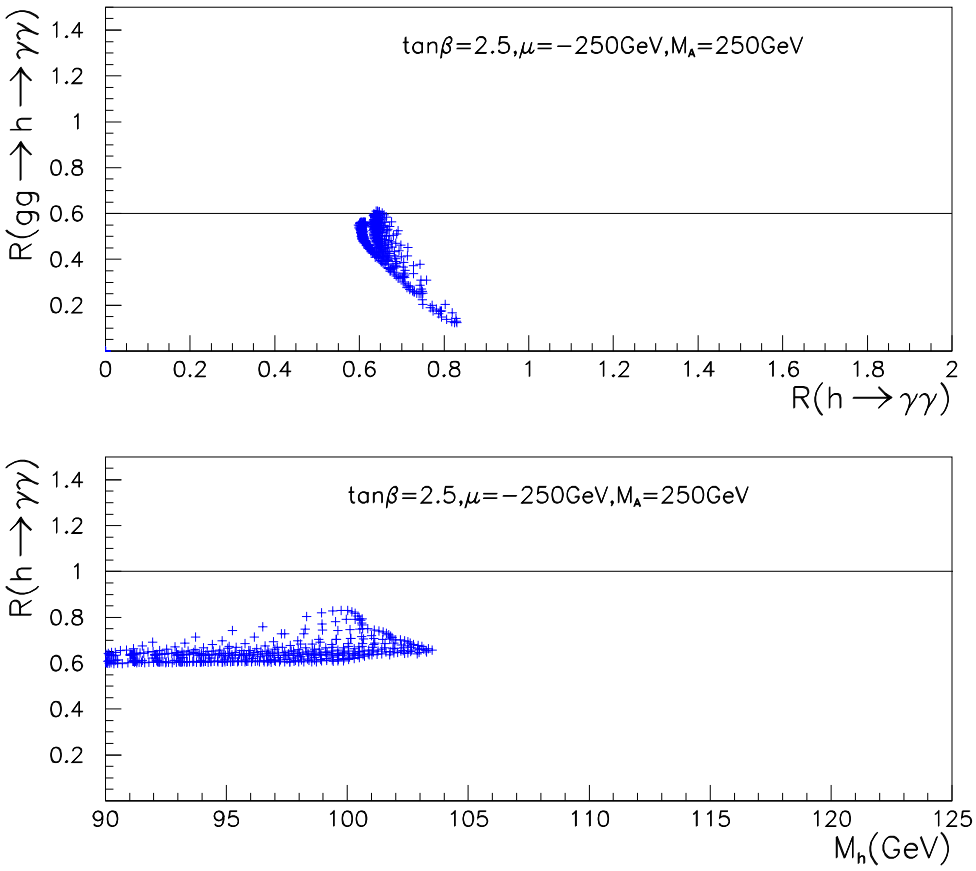

Figure 15: a) $R_{\gamma\gamma}$ *vs* M_h for $\tan\beta = 2.5, \mu = -250$ and $M_A = 250$TeV, with equal squark masses. b) As in a) but for $R_{gg\gamma\gamma}$ *vs* $R_{\gamma\gamma}$

below $2m_t$, one should also investigate direct $gg \to A, H$ production. A low mass $\tilde{t}_1$ has no effect either the production or decay (we are in scenario where $m_{\tilde{t}_2} > M_A$) of A, the usual channels should not be much affected. For H, one needs to critically review how the production is affected and whether $H \to \tilde{t}_1\tilde{t}_1$ can be exploited. The phenomenology is certainly richer here and the Higgs(es) should not be missed.

3.6 $\tan\beta = 5$

We now move to a larger $\tan\beta$. We go through basically the same steps as those in the previous section, 3.5. For the same scenarios we will scan over the same mass ranges. One general new feature will have to do with the fact that for larger $\tan\beta$ we obviously have larger Higgs masses. In most cases this will help. However on the whole similar conclusions will be reached.

3.6.1 The case of a common mass in the third generation squark sector with large M_A

Again $R_{gg\gamma\gamma}$ is most affected when the $\tilde{t}_1$ mass is smallest, Fig. 17. In the maximal mixing case, one new feature compared to $\tan\beta = 2.5$ is that the ratio $R_{gg\gamma\gamma}$ can be larger than one, for small $m_{\tilde{t}_1}$, reaching almost ~ 1.3. This is even more welcome that it occurs for Higgs masses in the range $92-98$GeV, Fig. 17. As a matter of fact, this is consistent with the argument we gave earlier: in this case $\tilde{t}_2$ is not too heavy so that the top and $\tilde{t}_1$ loop interfere and since the scale in the stop sector is not too high, the radiative corrections to the lightest Higgs mass are far from maximal. Considering that, especially in the lower end of this range, the significance in the direct channel are usually ($\mathcal{SM}$ or no-mixing) smallest, such scenarios can make it easier to discover h even in the direct channel. Of course, light $\tilde{t}_1$ (with much heavier $\tilde{t}_2$) can also lead to a much reduced $R_{gg\gamma\gamma}$. When this happens it occurs for higher Higgs masses, clustered around $M_h = 115$GeV. Though for this range of m_h significances in the direct production are much better, for certain values of the parameters the drop is too severe: $R_{gg\gamma\gamma} < .4$. But again this occurs simultaneously with an enhanced $R_{\gamma\gamma}$: $R_{\gamma\gamma} > 1.2$, Fig. 18. Again the smaller $R_{gg\gamma\gamma}$ the larger $R_{\gamma\gamma}$. As with the lower $\tan\beta$ when the direct production drops, $\sigma(pp \to \tilde{t}_1\tilde{t}_1 h)$ increases. When $R_{gg\gamma\gamma} < .6$ this cross section is in excess of 100fb up to $\simeq$ 650fb, for the smallest value of $R_{gg\gamma\gamma}$, Fig. 19. Note also that when $R_{gg\gamma\gamma} > 1$ this additional cross section is below 100fb.

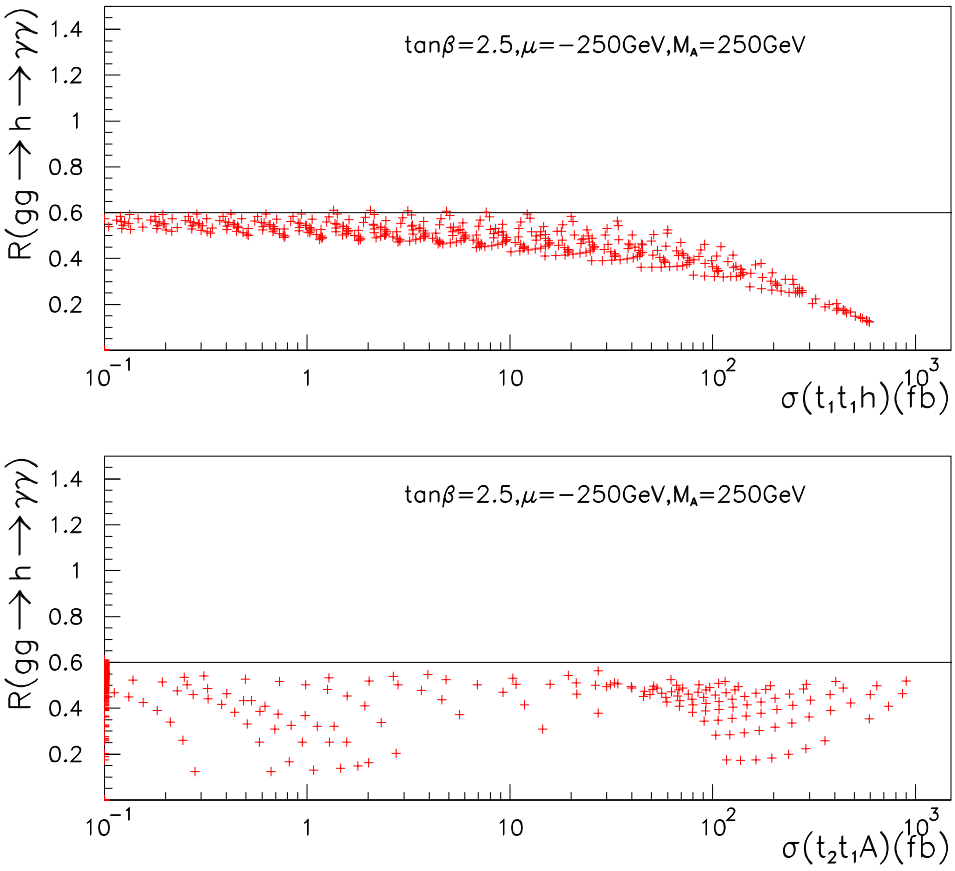

Figure 16: *As in Fig. 16 but for* $R_{\gamma\gamma}$ *vs* $\sigma(\tilde{t}_1\tilde{t}_1 h)$ *and* $\sigma(\tilde{t}_2\tilde{t}_1 A)$.

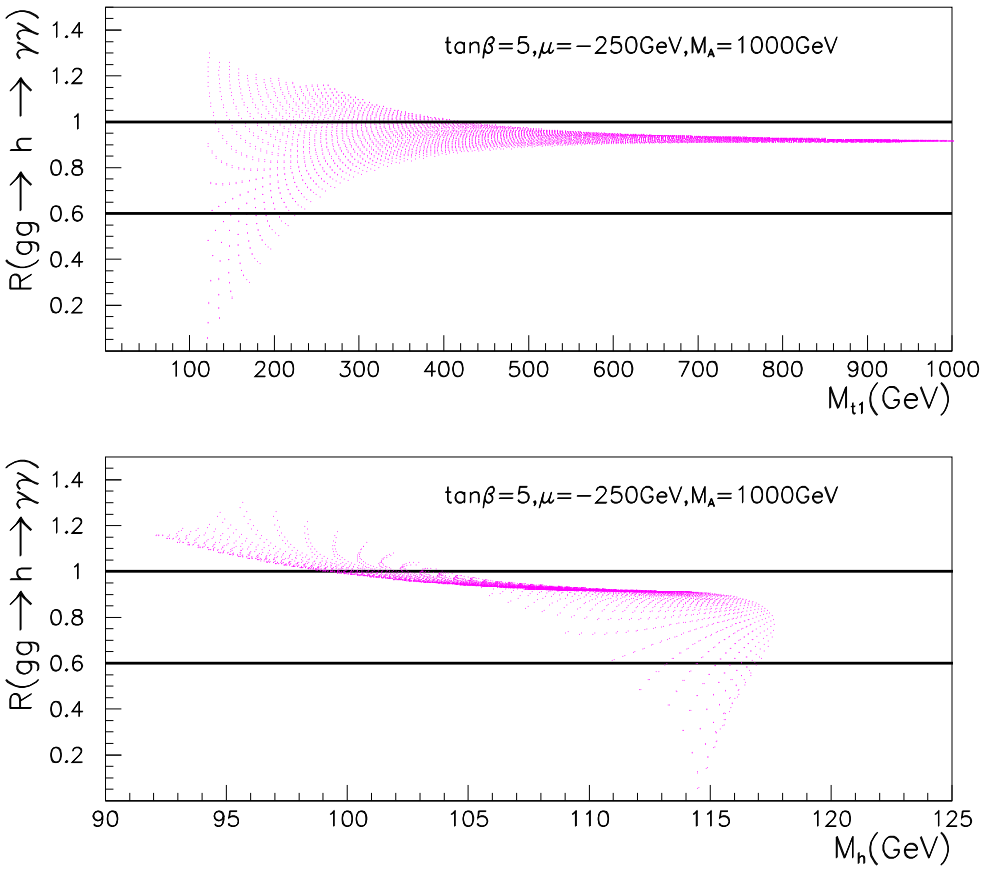

Figure 17: *a)* $R_{gg\gamma\gamma}$ *vs* $m_{\tilde{t}_1}$ *for* $\tan\beta = 5, \mu = -250\,GeV$ *and* $M_A = 1\,TeV$. *b) As in a) but for* $R_{gg\gamma\gamma}$ *vs* M_h .

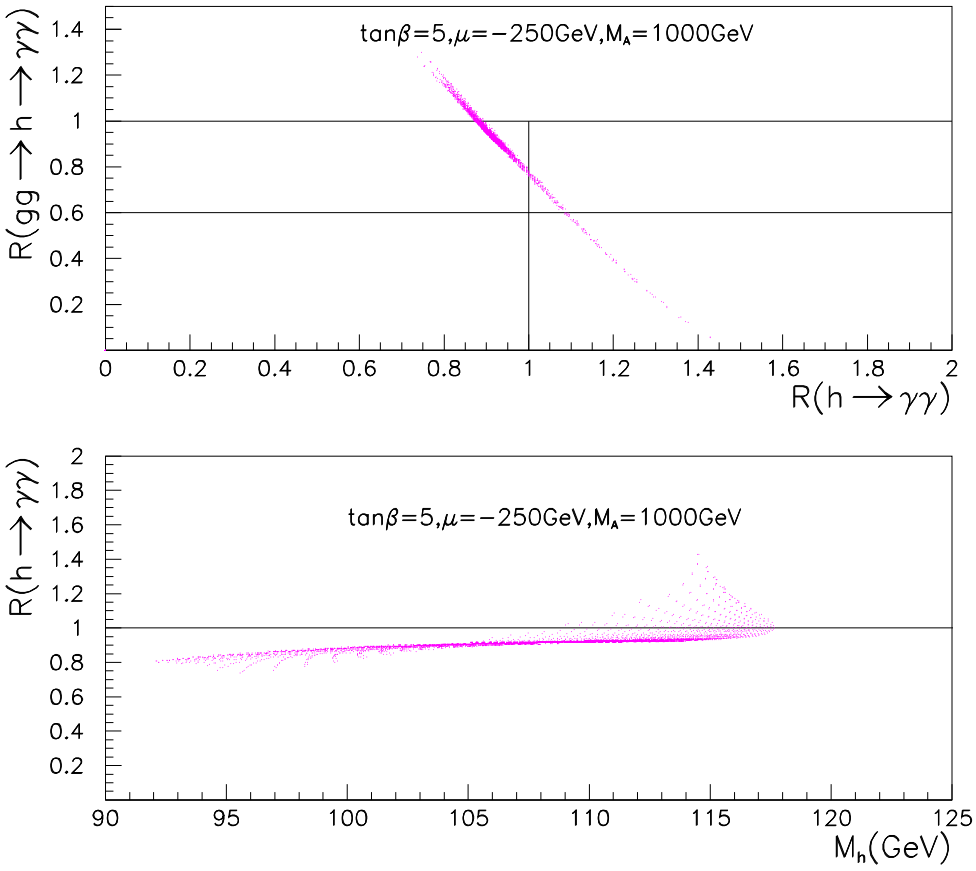

Figure 18: *a) As in Fig. 17 but for $R_{gg\gamma\gamma}$ vs $R_{\gamma\gamma}$. b) As in a) but for $R_{\gamma\gamma}$ vs M_h .*

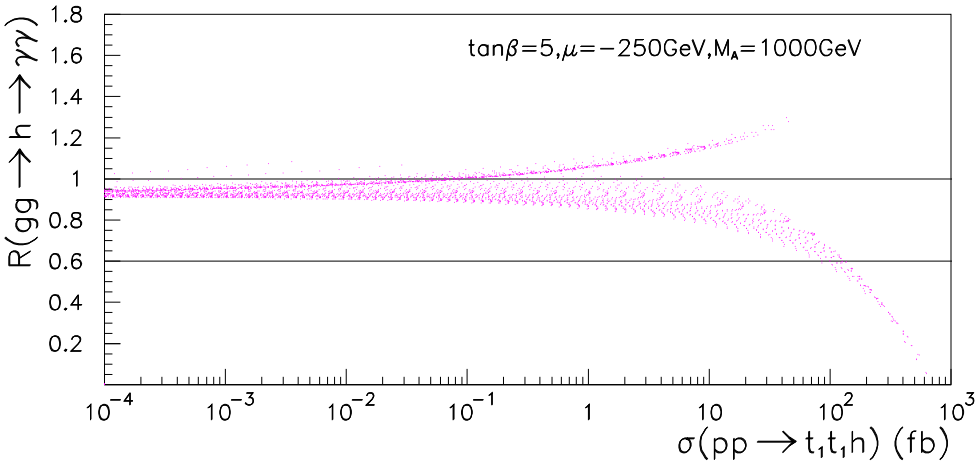

Figure 19: *As in Fig. 17 but for* $R_{\gamma\gamma}$ *vs* $\sigma(\tilde{t}_1\tilde{t}_1 h)$.

3.6.2 The case of a common mass in the third generation squark sector with $M_A = 350$GeV

The discussion is essentially the same as the one we presented for $\tan\beta = 2.5$ with $M_A = 350$GeV. The overall reduction factor from the lowering of M_A which affects $R_{\gamma\gamma}$ is slighty smaller (about .76) but then the reductions in $R_{gg\gamma\gamma}$ are for $m_h \sim 115$GeV, Fig. 20. Note also that $\sigma(\tilde{t}_1\tilde{t}_1 h)$ production, Fig. 21, is only slightly smaller than with $\tan\beta = 2.5$ (this is due to a higher Higgs mass) and therefore is a useful addition when the direct channel drops too much. For $R_{gg\gamma\gamma} < .2$ one gets as much as 400fb. For larger $\tan\beta$ and small M_A, de-excitation of $\tilde{t}_2$ into $\tilde{t}_1$ is not as efficient as for the lower $\tan\beta$ with the rather moderate values of μ that we have considered in this study. This is evident from Eq. 3.23, but as we see $\tilde{t}_1\tilde{t}_1 h$ still plays its role.

3.6.3 Lifting the degeneracy in the third family scalar masses

Taking unequal masses as in section 3.5.3, the reductions in the direct production are less pronounced. We do not get below $R_{gg\gamma\gamma} < .55$, while values up to 1.25 are still possible for $R_{gg\gamma\gamma}$. There is also little change in where these reductions or enhancements occur as a function of the Higgs mass. Again when $R_{gg\gamma\gamma} < .8$, $R_{\gamma\gamma} > 1$, Fig. 22. As with $\tan\beta = 2.5$ when the mass degeneracy is lifted, the channel $\tilde{t}_2 \to \tilde{t}_1 h$ opens up.This leads to typical cross sections of the order of 100fb especially for regions where the drop in the direct inclusive two-photon channel is the largest, see Fig. 22. This cross section can be larger

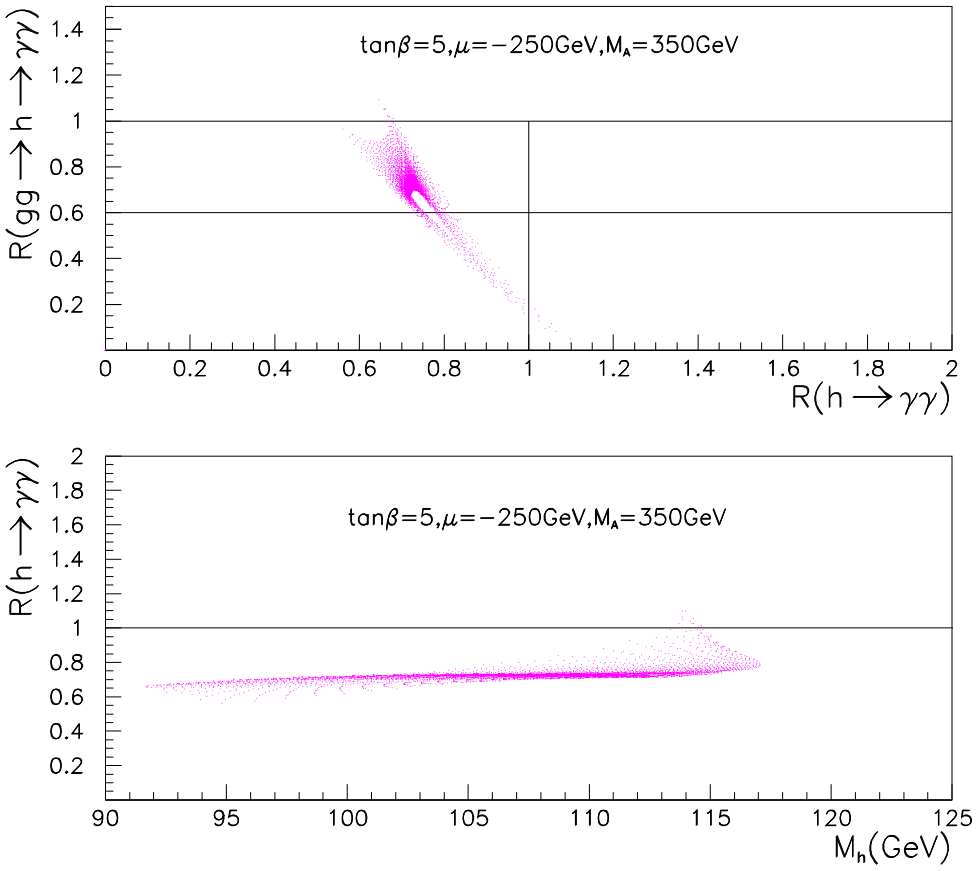

Figure 20: *a) As in Fig. 18 but for $R_{gg\gamma\gamma}$ vs $R_{\gamma\gamma}$. b) As in a) but for $R_{\gamma\gamma}$ vs M_h .*

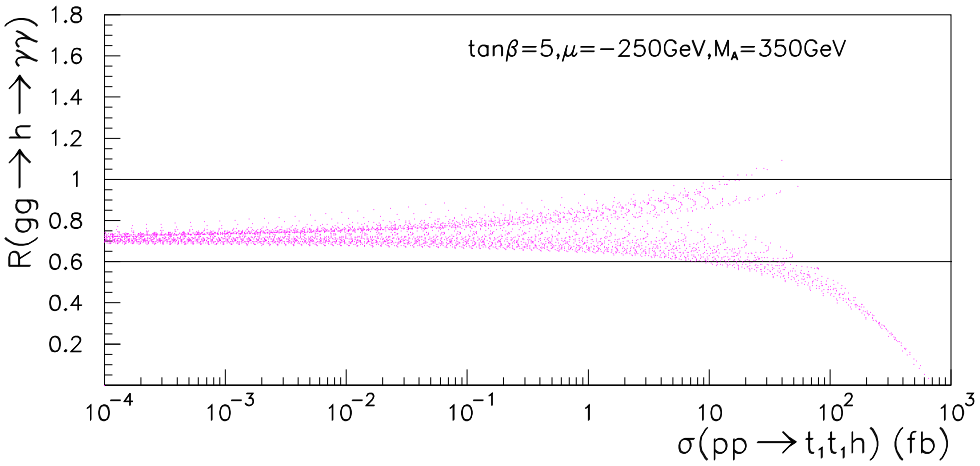

Figure 21: *As in Fig. 17 but for* $R_{\gamma\gamma}$ *vs* $\sigma(\tilde{t}_1\tilde{t}_1 h)$.

than 1pb in situation where $R_{gg\gamma\gamma}$ is little reduced. Of course our scans do show some regions where this cross section is unusable, typically when the mixing and stop splitting is small, but then as Fig. 22 shows the inclusive two-photon channel is unaffected. Of course continuum $\sigma(\tilde{t}_1\tilde{t}_1^* h)$ is still useful when large drops occurs (it is then around 100fb) but note that for our choice of parameters $\sigma(\tilde{t}_2\tilde{t}_1^* h)$ is practically always larger, Fig. 23.

3.7 $\tan\beta = 10$

Apart from the location, in terms of the Higgs mass, of where the largest drop in $R_{gg\gamma\gamma}$ occurs, that is around 118GeV, all the general features we found in the case with $\tan\beta = 5$ are recovered again, Figs. 24. Note that we do not get more noticeable reduction either in $R_{gg\gamma\gamma}$ or $R_{\gamma\gamma}$ due to the larger $\tan\beta$, and also that $R_{gg\gamma\gamma} > 1$ are possible. Similar observations to those made for $\tan\beta = 5$ can be made here even when we consider different splitting and lowering of masses, especially as concerns the importance of $\tilde{t}_2\tilde{t}_1^* h$. Some of these results are summarised in Figs. 24 .

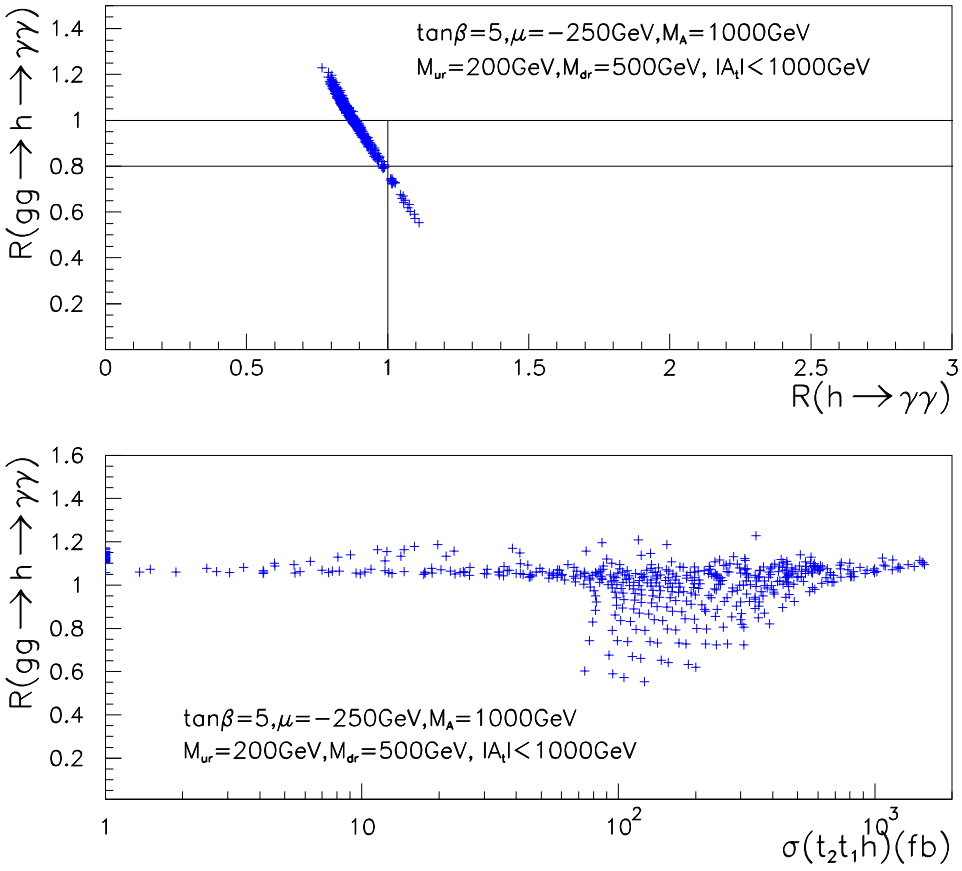

Figure 22: a) $R_{gg\gamma\gamma}$ *vs* $R_{\gamma\gamma}$ for $\tan\beta = 5, \mu = -250$GeV and $M_A = 1$TeV, when we allow different scalar masses for the third generation as given, see text . b) As in a) but for $R_{gg\gamma\gamma}$ *vs* $\tilde{t}_2\tilde{t}_1 h$

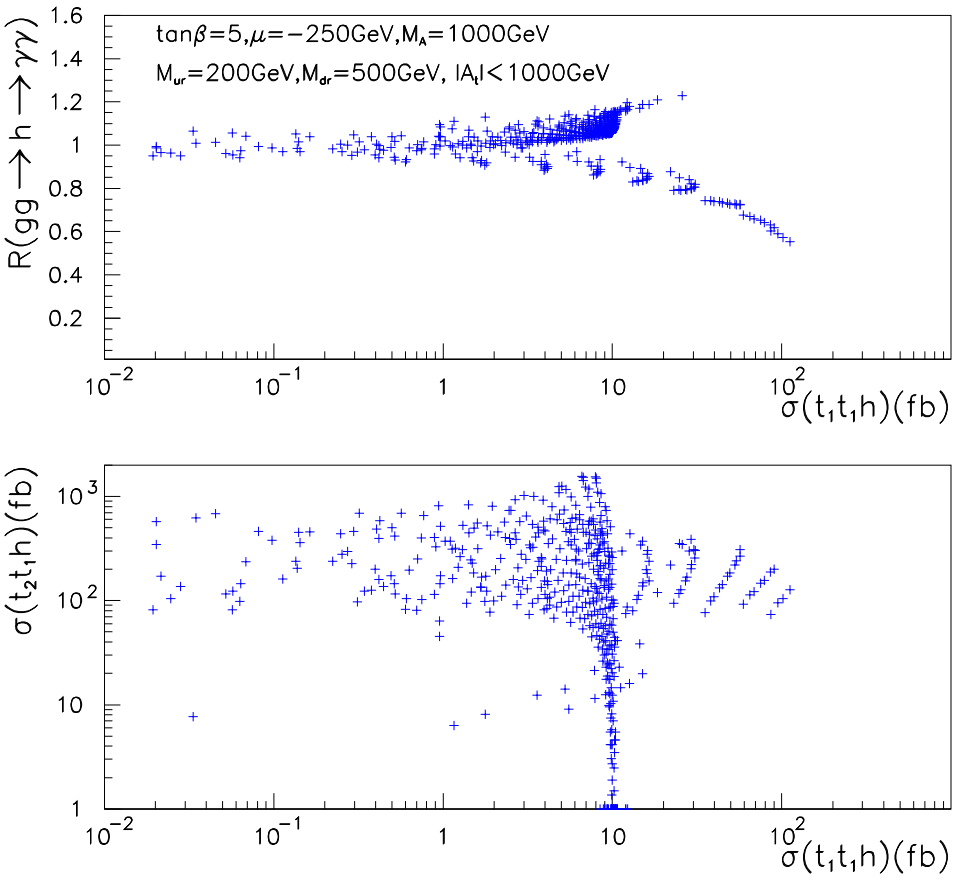

Figure 23: *As in Fig. 22 but for* $R_{gg\gamma\gamma}$ *vs* $\tilde{t}_1\tilde{t}_1h$ *and* $\tilde{t}_2\tilde{t}_1h$ *vs* $\tilde{t}_2\tilde{t}_1h$.

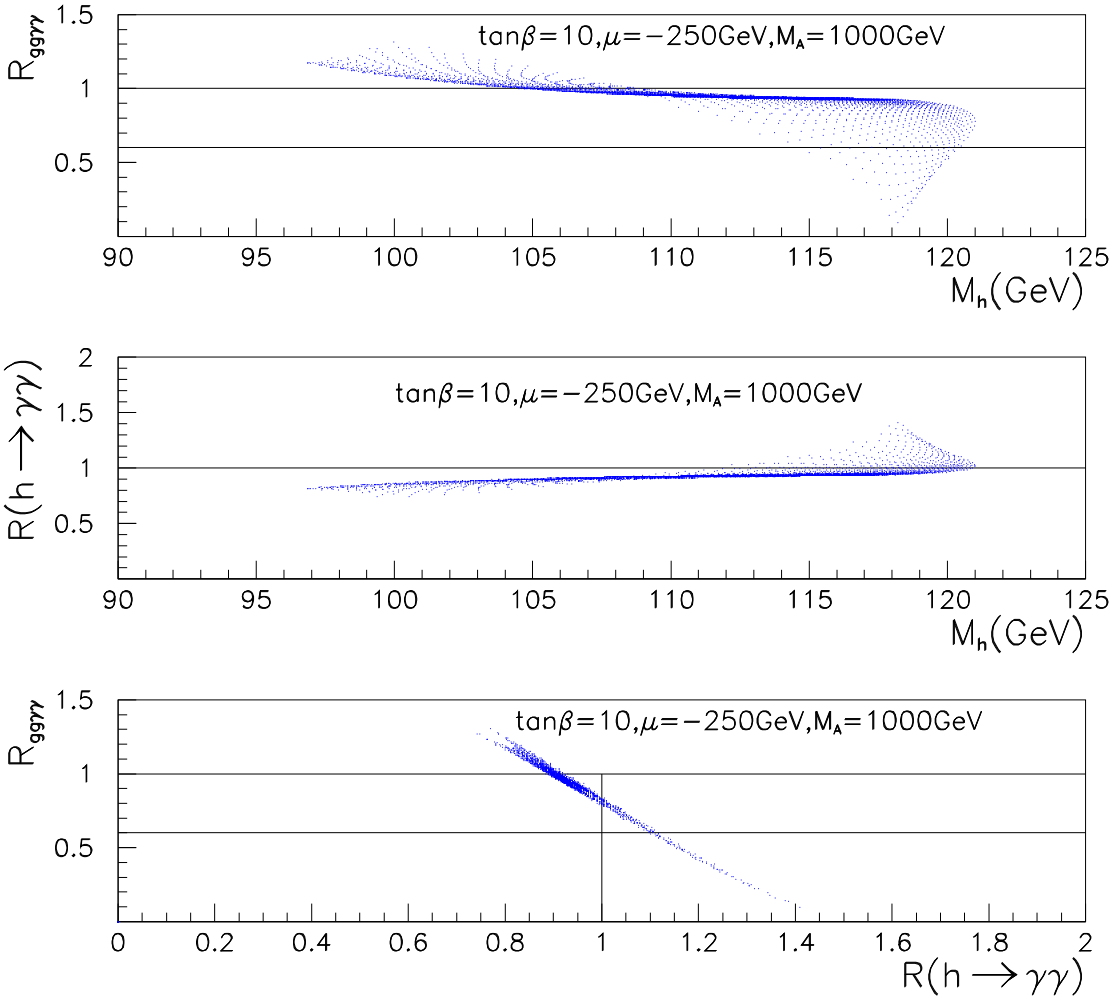

Figure 24: a) $R_{gg\gamma\gamma}$ *vs* m_h for $\tan\beta = 10, \mu = -250\text{GeV}$ and $M_A = 1\text{TeV}$, b) As in a) but for $R_{h\to\gamma\gamma}$ *vs* M_h , c) As in a) but for $R_{gg\gamma\gamma}$ *vs* $R_{\gamma\gamma}$

4 Conclusions

We have in this paper reinvestigated the fate of the photon signal of the lightest SUSY Higgs at the LHC when large tri-linear mixing terms in the stop sector are present. Previous investigations[7, 9] had drawn a very pessimistic picture of these scenarios. Our analysis shows that if we exploit all the consequences of these scenarios and not pick out only the Higgs signal in the inclusive channel these models have an excellent discovery potential. First, the large reductions in the inclusive two-photon signal not only require large mixing but also that one of the stops be relatively light. Although this has not been stressed in the text, a first signal of these scenarios will be $\tilde{t}_1\tilde{t}_1^*$ production with a cross section of order $\sim$ 100pb. Even though it may be argued that regions with the largest drops in the inclusive two-photon channel correspond to a very light stop and are likely to lead to a signature, jets+$\not{p}_T$, which is difficult. In any case it should be stressed that a hallmark of these scenarios is that whenever the signal in the inclusive channel drops that in the associated Wh/Zh and $t\bar{t}h$ channels increases and makes it up for the drop in the former channel. Moreover when $\sigma(pp \to h \to \gamma\gamma)$ gets too small the continuum $pp \to \tilde{t}_1\tilde{t}_1 h$ [24] reaches values of order few 100fb. More importantly we find that since these situations imply a large mass splitting between the two stops, $\tilde{t}_2 \to \tilde{t}_1 h$ can be substantial leading to another source of Higgs production with a yield larger than in the continuum and with a better signature than the $\tilde{t}_1\tilde{t}_1^* h$ continuum. We have shown that $\tilde{t}_2 \to \tilde{t}_1^* h$ occurs whenever the stop mixing angle does not take its maximal value, $|\sin 2\theta_{\tilde{t}}| = 1$, which is often unnaturaly assumed on the basis of equal soft SUSY breaking masses for the $SU(2)$ and $U(1)$ sfermions of the third generation, at the electroweak scale. We have also shown that although when M_A gets small the two-photon signals (both direct and associated) get further reduced (this happens even in the absence of mixing), with large tri-linear mixing terms and especially for low values of $\tan\beta$, one can trigger A production through the cascade $\tilde{t}_2 \to \tilde{t}_1 A$, beside the usual channels for A productions. Moreover one should not forget that especially with not too small $\tan\beta$, $\tan\beta > 3$, scenarios with light stops (but small mixing) do give an increase in the direct channel, but then an decrease in the associated two-photon channels. The overall conclusion we can draw almost resembles that of a no-lose scenario: whenever an effect reduces a particular signal it opens up new channels or enhances other channels. We have not discussed the use of $h \to b\bar{b}$ in the associated $t\bar{t}h$ channel which in these scenarios should allow detection. This requires rather good b-tagging facilities, as shown in [26]. This should certainly add to the discovery potential. The new associated stop Higgs signatures deserve a full simulation to critically quantify how beneficial these additions can be. In general there is a lack of detailed study of stop phenomenology at the LHC despite some important theoretical issues related to the third generation sfermions. As has been pointed out by several authors [51] the idea

of an inverted hierarchy of the SUSY spectrum whereby the third generation sfermions are, at the electroweak scale, much lighter than the first two is compelling and quite plausible. This helps solve the flavour problem in SUSY since very large masses for the superpartners of the first two generations can suppress FCNC, contributions to electric dipole moments and lepton flavour violations. This would still not go against naturalness since these particles couple weakly to the Higgs, at the heart of the fine-tuning problem. Naturalness does on the other hand require the stops and sbottoms (and the electroweak gauginos higgsinos) to be rather light, like in the scenarios we have studied and could also with a light stop make electroweak baryogenesis[52] work.

Acknowledgments

We would like to thank Guillaume Eynard for providing with his programme for calculating the significance of the two-photon associated Higgs signal using the ATLAS simulation and for very useful discussions. We also thank Michael Spira for promptly providing us with the code for the NLO stop pair production at the hadron colliders and Andrei Semenov for advice on the use of `CompHep`. We are also grateful to Elzbieta Richter-Waş for helpful discussions and communication,as well as providing us with an advance copy of the ATLAS TDR on Higgs Physics. K.S. acknowledges the hospitality of LAPTH where part of this work was done. This work is done under partial financial support of the Indo-French Collaboration IFCPAR-1701-1 *Collider Physics*.

References

[1] The limit on the mass of the SUSY Higgs depends on the SUSY parameters. For an update on the limits on the Higgs mass see:
F. Gianotti, Opal talk for the LEP Committee, March 1999,
`http://alephwww.cern.ch/ALPUB/seminar/lepc_mar99.pdf`.
N.J. Kjaer, Delphi talk for the LEP Committee, March 1999,
`http://delphiwww.cern.ch/delfigs/figures/niels990324.ps.gz`.
G. Bobbink, L3 talk for the LEP Committee, March 1999,
`http://l3www.cern.ch/conferences/ps/Bobbink_LEPC9903.ps`.
D. A.Glenzinski, Opal talk for the LEP Committee, March 1999,
`http://www1.cern.ch/Opal/plots/glenzinski/main.ps.gz`.

[2] J. F. Gunion, H.E. Haber, G.L. Kane and S. Dawson, *The Higgs Hunter's Guide*, Addison-Wesley, Reading, MA, USA, 1990.

[3] R.K. Ellis, I. Hinchliffe, M. Soldate and J. J . van der Bij, Nucl. Phys. **B297** (1988) 221.
J. Gunion, G. Kane and J. Wudka, Nucl. Phys. **B299** (1988) 231.

[4] J. Gunion and H. Haber, Nucl. Phys. **B278** (1986) 449.
H. Baer, D. Dicus, M. Drees and X. Tata, Phys. Rev. **D36** (1987) 1363.
K. Griest and H. Haber, Phys. Rev. **D37** (1988) 37.
H. Baer, M. Bisset, D. Dicus, C. Kao and X. Tata, Phys. Rev. **D47** (1992) 1062.
A. Djouadi, J. Kalinowski and P. M. Zerwas,Z. Phys. **C57** (1993) 569.

[5] H. Baer, M. Bisset, C. Kao and X. Tata, Phys. Rev. **D46** (1992) 1067.

[6] H. Baer, M. Bisset, D. Dicus, C. Kao and X. Tata, Phys. Rev. **D47** (1992) 1062.

[7] B. Kileng, Z. Phys. **C63** (1993) 87.
B. Kileng, P. Osland, P.N. Pandita, Z.Phys. **C71** (1996)87. hep-ph/9506455.

[8] G. L Kane, G. D. Kribs, S.P Martin and J. D. Wells, Phys. Rev. **D50** (1996) 213.

[9] A. Djouadi, Phys.Lett. **B435** (1998) 101, hep-ph/9806315.

[10] Z. Kunszt and F. Zwirner, Nucl. Phys. **B385** (1992) 3.

[11] E. Richter-Wąs et al., ATLAS Internal note, PHYS-No-074 (1996).

[12] For an update on the Higgs analysis in ATLAS see, the ATLAS Technical Design Report, the ATLS Collaboration, 1999, to appear.
`http://atlasinfo.cern.ch/Atlas/GROUPS/PHYSICS/HIGGS/higgs-www/Analyses-notes.html/higgs-sugra.ps.gz`.

[13] For an update on Higss searches in CMS see, R. Kinnunen and D. Denegri, CMS Note 1997/057, April 1997.

[14] For a review see, H.P. Nilles, Phys. Rep. **110** (1984) 1.
R. Arnowitt, A. Chamseddine and P. Nath, *Applied N=1 Supergravity*, World Scientific, 1984.

[15] H. Baer, M. Bisset C. Kao and X. Tata, Phys. Rev. **D50** (1993) 316.

[16] G. Polesello, L. Poggioli, E. Richter-Wąs and J. Sderqvist, ATLAS Internal Note, PHYS-No-111, Oct. 1997.

[17] H. Haber, in *Perspectives in Higgs Physics II*, ed. G.L. Kane, World Scientific, Singapore, 1998.

[18] S. L. Glashow, D.V. Nanopoulos and A. Yildiz, Phys. Rev. **D18** (1978) 1724.

[19] Z. Kunszt, Nucl. Phys. **B247** (1984) 339.
J. F. Gunion et al., Nucl. Phys. **B294** (1987) 621.
D. Dicus and S.S.D. Willenbrock, Phys. Rev. **D39** (1989) 751.
W. Marciano and F. Paige, Phys. Rev. Lett. **66** (1991) 2433.
J. Gunion, Phys. Lett. **B 261** (1991) 510.
The K-factor for WH in the SM is calculated in T. Han and S.S.D. Willenbrock, Phys. Lett. **B273** (1990) 167.

[20] J. Gunion and L. Orr, Phys. Rev. **D46** (1992) 2052.

[21] S. Abdullin, A. Starodumov and N. Stepanov, CMS TN/93-86 (1993).
M. Dzelayin, Z. Antunovic, D. Denegri and R. Kinnunen, CMS TN/96-091 (1996).

[22] For a detailed analysis of the two-photon signal in the associated production in ATLAS see, G. Eynard, Ph. D thesis, LAPP-T-98/02, LAPP-Annecy, May 1998.

[23] D. Froidevaux, F. Gianotti and E. Richter-Wąs, ATLAS Internal Note, PHYS-No-64, Feb. 1995.

[24] For a study of stop stop Higgs production at the LHC see, A. Djouadi and J. L. Kneur and G. Moultaka, Phys. Rev. Lett. **80** (1998) 1830.hep-ph/9711244; *ibid* hep-ph/9903218.

[25] J. Dai, J. F. Gunion and R. Vega, Phys. Rev. Lett. **71** (1993) 2699.

[26] D. Froidevaux and E. Richter-Wąs, ATLAS Internal Note, PHYS-No-043, Sep. 1994.

[27] V. Drollinger, T. Mühler and R. Kinnunen, CMS Note 1998/003; *ibid* 1999/01.

[28] A. Djouadi, J. Kalinowski and M .Spira, Comp. Phys. Comm. **108** (1998) 56. hep-ph/9704448.

[29] M. Carena, J. R Espinosa, M. Quiros and C.E.M. Wagner, Phys. Lett. **355B** (1995) 209.
M. Carena, M. Quiros and C.E.M. Wagner, Nucl. Phys. **B461** (1996) 407.

[30] G. Bélanger, F. Boudjema, T. Kon and V. Lafage, hep-ph/9711334,Eur. J. Phys., in Press.

[31] W. Loinaz and J. D. Wells, Phys. Lett. **B445** (1998) 178. hep-ph/9808287.

[32] H. Baer, J. D. Wells, Phys.Rev.**D57** 4446 (1998). hep-ph/9710368.

[33] M. Carena, S. Mrenna and C.E.M. Wagner, Preprint ANL-HEP-PR-98-54, CERN-TH/98-262, FERMILAB-PUB-98/250-T, Sep. 1998. hep-ph/9808312.

[34] M. M. Nojiri, Phys. Rev. **D51** (1995) 6281.
M.M. Nojiri, K. Fujii and T. Tsukamoto, Phys. Rev. **D54** (1996) 6756.

[35] For a compendium on the phenomenology of third generation sfermions see, W. Porod, Ph.D Thesis, Wien Uni.1998. hp-ph/9804208.

[36] For a description of `CompHep`, see E.Boos et al., Proc.of the XXVIth Rencontres de Moriond, ed.by J.Tran Thanh Van, Editions Frontiers, 1991, p.501; E.Boos et al., Proc. of the Int. Conf. on Computing in High Energy Physics, ed.by Y.Watase, F.Abe, Universal Academy Press, Tokyo, 1991, p.391; E.Boos et al., Int. J. Mod. Phys. **C5** (1994) 615; E.Boos et al., SNU CTP preprint 94-116, Seoul, 1994 (hep-ph/9503280).

[37] A. Dedes and S. Moretti, preprint RAL-TR-1998-081, Dec. 1998.hep-ph/9812328,.

[38] Z. Kunszt, S. Moretti and W.J. Stirling, Z. Phys. **C74** (1997) 479.

[39] W. Beenakker *et al.*, Nucl.Phys. **B515** (1998) 3. hep-ph/9710451.
For review on QCD corrections to SUSY particles production at hadron colliders, see T. Plehn, Doctoral thesis, DESY-THESIS-1998-024, Jul 1998. hep-ph/9809319.

[40] A. Bartl, W. Majerotto and W. Porod, Z. Phys. **C64** (1994) 499; erratum *ibid* **C68** (1995) 518.
A. Bartl *et al.,* Z. Phys. **C73** (1997) 549; *ibid* **C76** (1997) 469.
A. Bartl *et al.,*, Phys. Lett. **B435** (1998) 118.

[41] For a description of the program see for example M. Jimbo and H. Tanaka and T. Kaneko and T. Kon, hep-ph/9503363.
J. Fujimoto et al., Comp. Phys. Commun. **111** (1998) 185. hep-ph/9711283.

[42] S. Kraml, *Stop and Sbottom Phenomenology in the MSSM*, Ph.D Thesis, Univ. of Vienna. hep-ph/9903257. This has a nice review of QCD corrections to stop decays.

[43] M. Drees and K. Hagiwara, Phys. Rev. **D42** (1990) 1709.
R. Barbieri, M. Frigeni, F. Giuliani and H.E. Haber, Nucl. Phys. **B341** (1990) 309.
M. Drees and K. Hagiwara and A. Yamada, Phys. Rev. **D45** (1992) 1725.
D. Garcia and J. Solà, Mod. Phys. Lett. **A9** (1994) 211.
P.H. Chankowski *et al.,* Nucl. Phys. **B417** (1994) 101.
For earlier analyses see, R. Barbieri and L. Maiani, Nucl. Phys. **B224** (1983) 32.
C.S. Lim, T. Inami and N. Sakai, Phys. Rev. **D29** (1984) 1488.

Z. Hioki, Prog. Theor. Phys. **73** (1985) 1283.
J. A. Grifols and J. Solà, Nucl. Phys. **B253** (1985) 47.

[44] J. Erler and P. Langacker, hep-ph/9809352.

[45] A. Djouadi *et al.*, Phys. Rev. Lett. **78** (1997) 3626; Phys. Rev. **D57** (1998) 4179.

[46] J.M. Frère, D.R.T Jones and S. Raby, Nucl. Phys. **B222** (1983) 11.
M. Claudson, L. Hall and I. Hinchcliffe, Nucl. Phys. **B228** (1983) 501.
C. Kounnas, A.B. Lahanas, D.V. Nanopoulos and M. Quirós, Nucl. Phys. **B236** (1984) 438.
J.F. Gunion, H.E. Haber and M. Sher, Nucl. Phys. **B306** (1988) 1.
P. Langacker and N. Polonsky, Phys. Rev. **D50** (1994) 5824.
A. Strumia, Nucl. Phys. **B482** (1996) 24.
For a recent summary see, J. A. Casas, to be published in *Perspectives on Supersymmetry*, ed. G. L. Kane, World scientific. hep-ph/9707475.

[47] A. Kusenko, P. Langacker and G. Segre, Phys. Rev. **D54** (1996) 5824. hep-ph/9602414.
A. Kusenko and P. Langacker, Phys. Lett. **391** (1997) 29. hep-ph/9608340.
A. Kusenko, Nucl. Phys. Proc. Suppl. **52A** (1997) 67. hep-ph/9607287.

[48] C. M. Holck (CDF Coll.), Abstract 652, ICHEP 98, Vancouver, BC, July 98.

[49] K. Hikasa and M.Kobayashi, Phys. Rev. **D36** (1987) 724.

[50] See for instance, M. Drees and M.M. Nojiri, Nucl. Phys. **B369** (1992) 54.
M. Drees and and S.P. Martin, hep-ph/9504324.
V. Barger, M.S. Berger and P. Ohmann, Phys. Rev. **D47** (1993) 1093.
D.J. Castano, E.J. Piard and P. Ramond, Phys. Rev. **D49** (1994) 4882.
M. Carena, M. Olechowski, S. Pokorski and C.E.M Wagner, Nucl. Phys. **B419** (1994) 213; M. Carena and C.E.M Wagner, Nucl. Phys. **B452** (1995) 45.

[51] S. Dimopoulos and G. F. Giudice, Phys. Lett.]bf 357 (1995) 573.
A. Pomarol and D. Tommasini, Nucl. Phys. **B466** (1996) 3.
G. Dvali and A. Pomarol, Phys. Rev. Lett. **77** (1996) 3728; *ibid*Nucl. Phys. **B522** (1998) 3.
A. G. Cohen, D.B. Kaplan and A. E. Nelson, Phys. Lett. **B388** (1996) 588.
J.L. Feng, C. Kolda and N. Polonsky, hep-ph/9810500.

[52] See for instance,J. R Espinosa, Nucl. Phys. **B475** (1996) 273.
J.M. Cline, M. Joyce and K. Kainulainen, Phys. Lett. **B417** (1998) 79.hep-ph/9708393.

M. Carena, M. Quirós and C.E.M. Wagner, Nucl. Phys. **B524** (1998) 3. hep-ph/9710401.
J.M. Moreno, M. Quirós and M. Seco, Nucl. Phys. **B526** (1998) 489. hep-ph/9801272.
M. Laine and K. Rummukainen, Phys. Rev. Lett. **80** (1998) 5259. hep-ph/9804255.
J.M. Cline, Preprint McGill-98/27. hep-ph/9810267.